L-MT-15-074

ENCLOSURE 6

WESTINGHOUSE WCAP-17549-NP, (NON-PROPRIETARY) REVISION 3

MONTICELLO REPLACEMENT STEAM DRYER STRUCTURAL EVALUATION FOR HIGH-CYCLE ACOUSTIC LOADS USING ACE

90 pages follow

Westinghouse Non-Proprietary Class 3

WCAP-17549-NP
Revision 3

October 2015

Monticello Replacement Steam Dryer Structural Evaluation for High-Cycle Acoustic Loads Using ACE

WCAP-17549-NP
Revision 3

Monticello Replacement Steam Dryer Structural Evaluation for High-Cycle Acoustic Loads Using ACE

Yan Han*

Reviewed by Amir Salehzadeh*

BWR Engineering

October 2015

Approved: **Sanjaybir S. Bakshi*, Manager**
BWR Engineering

*Electronically approved records are authenticated in the electronic document management system.

Westinghouse Electric Company LLC
1000 Westinghouse Drive
Cranberry Township, PA 16066

© 2015 Westinghouse Electric Company LLC
All Rights Reserved

Record of Revisions		
Rev	**Date**	**Revision Description**
0	May 2012	Acoustic load input developed with [ ]^{a,c} (per WCAP-17540-P Rev. 0)
1	March 2013	Acoustic load input developed with [ ]^{a,c} (per WCAP-17716-P Rev. 0)
2	August 2013	Acoustic load input developed with [ ]^{a,c} (per WCAP-17716-P Rev. 1)
3	See EDMS	Add Appendix B for acoustic load input developed per WCAP-17252 Rev.5. This documents the updated high-cycle fatigue stress ratios that were evaluated from this latest plant EPU data. Change bars are used throughout the document to show the modifications from the previous version of this document.

TABLE OF CONTENTS

1 INTRODUCTION 1-1

2 METHODOLOGY 2-1

2.1 ACOUSTIC LOAD ANALYSIS 2-1

2.1.1 Overview 2-1

2.1.2 Design Requirements 2-1

2.1.3 Dryer Geometry 2-2

2.2 [ ]^{a,c} 2-2

3 FINITE ELEMENT MODEL DESCRIPTION 3-1

3.1 STEAM DRYER GEOMETRY 3-1

3.2 FINITE ELEMENT MODEL MESH AND CONNECTIVITY 3-2

3.2.1 Mesh Density Study 3-2

3.2.2 Shell-Solid Connections in the FEM 3-3

3.2.3 Vane Bank Representation 3-3

3.2.4 Lifting Rod Representation 3-4

3.2.5 Beam – Solid Connections in the FEM 3-4

3.2.6 Dryer Skirt Submerged in Water 3-4

4 MATERIAL PROPERTIES 4-1

4.1 STRUCTURAL DAMPING 4-1

5 MODAL ANALYSIS 5-1

6 LOAD APPLICATION 6-1

7 STRUCTURAL ANALYSIS 7-1

7.1 HARMONIC ANALYSIS 7-1

7.1.1 [ ]^{a,c} 7-1

7.1.2 Overview – Time-History Solution 7-1

7.1.3 Inverse Fourier Transform 7-2

7.1.4 Frequency Scaling (Shifting) 7-3

7.2 POST-PROCESSING 7-4

7.2.1 Primary Stress Evaluation 7-4

7.2.2 Alternating Stress 7-4

7.3 CALCULATION AND EVALUATION OF WELD STRESSES 7-5

7.4 SUBMODELING TECHNIQUES 7-8

7.5 [ ]^{a,c} 7-9

8 ANALYSIS RESULTS 8-1

8.1 GLOBAL MODEL 8-1

8.2 SUBMODELING 8-1

8.2.1 [ ]^{a,c} 8-1
8.2.2 Submodel Mesh Density 8-1
8.3 ASME Alternating Stress Calculations 8-2
9 SUMMARY OF RESULTS AND CONCLUSIONS 9-1
10 REFERENCES 10-1
APPENDIX A SKIRT SLOT SUBMODEL MESH DENSITY STUDY A-1
APPENDIX B HIGH CYCLE FATIGUE STRESS RE-EVALUATION B-1

LIST OF TABLES

Table 2-1 Vane Passing Frequency [ ]^{c} 2-3

Table 2-2 Summary of Maximum Vane Passing Frequency Stress at EPU 2-3

Table 4-1 Summary of Material Properties 4-2

Table 4-2 Summary of Vane Bank [ ]^{a,b,c} 4-2

Table 8-1 Summary of Results at EPU: Components [ ]^{a,c} 8-3

Table 8-2 Summary of Results at EPU: Components [ ]^{a,c} 8-4

Table 8-3 ASME Alternating Stress Calculation Summary 8-4

Table A-1 Submodel Cut Boundary Stress Comparison A-2

Table A-2 Submodel Cut Boundary Stress Comparison A-2

Table B–1 Summary of Results at 2015 EPU: Components Above the Support Ring B-3

Table B–2 Summary of Results at 2015 EPU: Components Below the Support Ring B-3

LIST OF FIGURES

Figure 1-1 Schematic of Monticello Replacement Steam Dryer 1-2
Figure 2-1 Geometry Plot: [ ]^{a,c} 2-4
Figure 2-2 Geometry Plot: [ ]^{a,c} 2-5
Figure 2-3 Geometry Plot: [ ]^{a,c} 2-6
Figure 2-4 Geometry Plot: [ ]^{a,c} 2-7
Figure 2-5 Geometry Plot: [ ]^{a,c} 2-8
Figure 2-6 Geometry Plot: [ ]^{a,c} 2-9
Figure 2-7 Geometry Plot: [ ]^{a,c} 2-10
Figure 3-1 Monticello Replacement Steam Dryer Finite Element Model 3-5
Figure 3-2 Lower [ ]^{a,c} 3-6
Figure 3-3 Lower [ ]^{a,c} 3-7
Figure 3-4 Vane Bank Structural Components 3-8
Figure 3-5 Vane Bank Geometry 3-9
Figure 3-6 Dryer Hood Geometry 3-10
Figure 3-7 Skirt Geometry 3-11
Figure 3-8 [ ]^{a,c} 3-12
Figure 3-9 [ ]^{a,c} 3-13
Figure 3-10 [ ]^{a,c} 3-14
Figure 3-11 Lifting Rod Geometry 3-15
Figure 3-12 [ ]^{a,c} 3-16
Figure 3-13 [ ]^{a,c} 3-17
Figure 3-14 [ ]^{a,c} 3-18
Figure 3-15 [ ]^{a,c} 3-19
Figure 3-16 [ ]^{a,c} 3-20
Figure 3-17 Structural Components of Vane Bank 3-21
Figure 3-18 Structural and Non-Structural Components of Vane Bank 3-22
Figure 3-19 Vane Bank Mass Blocks 3-23
Figure 3-20 [ ]^{a,c} 3-24
Figure 5-1 Modal Analysis: [ ]^{a,c} 5-2
Figure 5-2 Modal Analysis: [ ]^{a,c} 5-3
Figure 5-3 Modal Analysis: [ ]^{a,c} 5-4

Figure 5-4 Modal Analysis: [ ]^{a,c} 5-5
Figure 6-1 [ ]^{a,c} 6-3
Figure 6-2 [ ]^{a,c} 6-4
Figure 6-3 [ ]^{a,c} 6-5
Figure 6-4 [ ]^{a,c} 6-6
Figure 8-1 [ ]^{a,c} 8-5
Figure 8-2 [ ]^{a,c} 8-6
Figure 8-3 [ ]^{a,c} 8-7
Figure 8-4 [ ]^{a,c} 8-8
Figure 8-5 [ ]^{a,c} 8-9
Figure 8-6 [ ]^{a,c} 8-10
Figure A-1 Submodel [ ]^{a,c} A-3
Figure A-2 Submodel Mesh Densities A-4
Figure A-3 [ ]^{a,c} Submodel Results A-5
Figure A-4 [ ]^{a,c} Submodel Results A-6
Figure A-5 [ ]^{a,c} Submodel Results A-7
Figure B-1 Outer Hood (non-weld) B-1
Figure B-2 Outer Hood to Cover Plate Weld B-2
Figure B-3 Skirt to Skirt Flange Weld B-2

EXECUTIVE SUMMARY

A high-cycle fatigue evaluation of the Westinghouse replacement steam dryer for the Monticello plant has been completed with loads generated using the Acoustic Circuit Enhanced (ACE) [ ]^{a,c} Acoustic loads and stresses for extended power uprate (EPU) conditions have been evaluated for high-cycle fatigue and have been determined to meet the American Society of Mechanical Engineers (ASME) Boiler and Pressure Vessel (B&PV) Code Section III, Subsection NG criteria.

[

]^{a,c}

[

]^{a,c}.

	Above Support Ring	Below Support Ring
Licensing Based Evaluation (based on 2011 CLTP data)	[ ]^{a,c}	[ ]^{a,c}
Power Ascension Test Results Evaluation (based on 2015 EPU data)	[ ]^{a,c}	[ ]^{a,c}

To account for uncertainties in the modal frequency predictions of the finite element model (FEM), the stresses are also computed for loads that are shifted in the frequency domain by[ ]^{a,c}. These results also include a conservative estimate of the high cycle fatigue stress caused by vane passing frequency (VPF) of the recirculation pumps.

LIST OF ABBREVIATIONS

Abbreviation	Description
ACE	acoustic circuit enhanced
ASME	American Society of Mechanical Engineers
B&PV	boiler and pressure vessel
BWR	boiling water reactor
CLTP	current licensed thermal power (1775 MWt)
EPU	extended power uprate (2004 MWt)
FEM	finite element model
FSRF	fatigue strength reduction factor
IFT	inverse Fourier transform
MPC	multi-point constraint
MSL	main steam line
MWt	megawatts thermal
SCF	stress concentration factor
[	]^{a,c}
VB	vane bank
VPF	vane passing frequency
2-D	two-dimensional
3-D	three-dimensional

Trademark Note:

ANSYS, ANSYS Workbench, CFX, AUTODYN, and any and all ANSYS, Inc. product and service names are registered trademarks or trademarks of ANSYS, Inc. or its subsidiaries located in the United States or other countries.

1 INTRODUCTION

In 2002, after increasing power to 117% of the original licensed thermal power, the steam dryer in a boiling water reactor (BWR) had a significant reduction in its structural integrity. After extensive evaluation by various industry experts, the root cause of the dryer degradation was determined to be acoustic fluctuating pressure loads on the dryer, resulting from resonances produced by steam flow in the main steam lines (MSLs) across safety and relief valve inlets. The degradation experienced in the steam dryer of a BWR led to changes to Regulatory Guide 1.20, requiring plants to evaluate their steam dryer before any planned increase in power level.

The Monticello power plant has contracted Westinghouse for a replacement steam dryer, and is also planning a power uprate. In conjunction with the component replacement by Monticello and the planned power uprate, an analysis has been performed to qualify the replacement steam dryer, shown in Figure 1-1, for acoustic pressure loads and vibratory loads caused by vane passing frequency of the recirculation pumps. The process used to perform the analysis involves [

]^{a,c} Acoustic loads, based on plant data taken at CLTP conditions, scaled to to EPU conditions are evaluated. A dynamic analysis is performed using [

]^{a,c}

a,c

Figure 1-1 Schematic of Monticello Replacement Steam Dryer

2 METHODOLOGY

2.1 ACOUSTIC LOAD ANALYSIS

2.1.1 Overview

An analysis has been performed to assess the structural integrity of the replacement dryer for the Monticello plant subject to acoustic loads. [

]^{a,c}

2.1.2 Design Requirements

2.1.2.1 [ ]^{a,c}

The replacement dryer is analyzed according to the 2004 Edition of the ASME B&PV Code, Subsection NG (Reference 1). This report documents the suitability of the replacement dryer for high-cycle fatigue loads resulting from acoustic loads and vane passing frequency loads due to the recirculation pumps. The governing criterion for the analysis is in terms of the allowable component fatigue usage. The objective of this analysis is to show that the maximum alternating stress intensity anywhere in the dryer is less than the material endurance strength at 10^{11} cycles. The applicable fatigue curve for stainless steel (the dryer is manufactured from SS316L), is shown in Figure I-9.2.2 in Appendix I of the ASME Code.

[

]^{a,c}

2.1.2.2 Young's Modulus Correction

Before comparing the maximum alternating stress intensity to the ASME Code endurance strength, it is necessary to account for the Young's modulus correction. The analysis uses a Young's modulus of 25.425 x 10^6 psi, compared to the value to construct the fatigue curves of 28.3 x 10^6 psi. The ratio that is applied to the calculated alternating stress intensities is 1.113 (28.3 / 25.425).

2.1.2.3 [ ]^{a,c}

[

]^{a,c}

2.1.3 Dryer Geometry

Plots showing various aspects of the dryer configuration are provided in Figures 2-1 through 2-7.

2.2 [ ]^{a,c}

[

]^{a,b,c}

[

]a,b,c

Table 2-1 Vane Passing Frequency [ ]c a,b,c

Table 2-2 Summary of Maximum Vane Passing Frequency Stress at EPU a,b,c

a,c

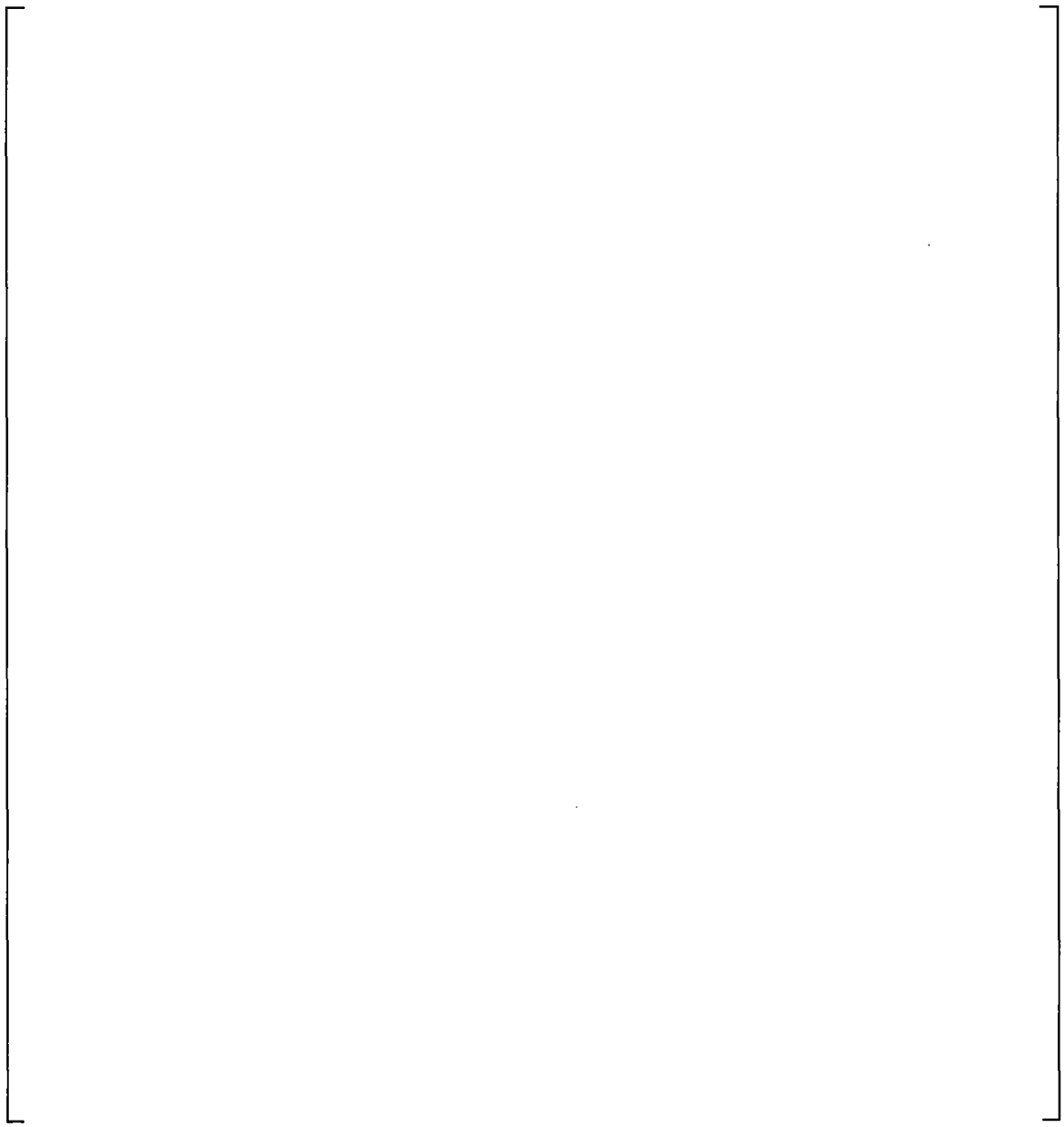

Figure 2-1 Geometry Plot: [ ]^{a,c}

a,c

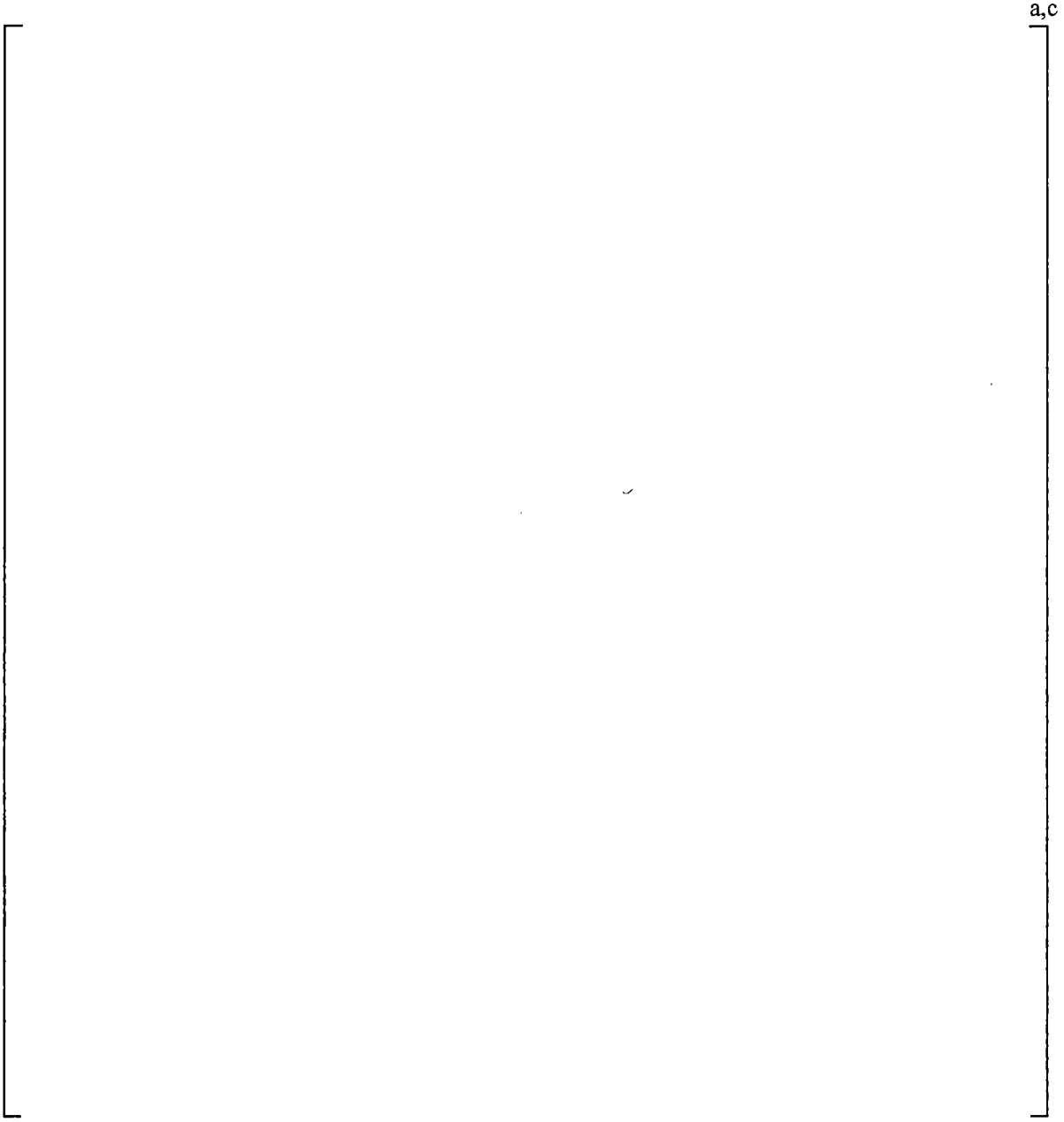

Figure 2-2 Geometry Plot: [ ]^{a,c}

a,c

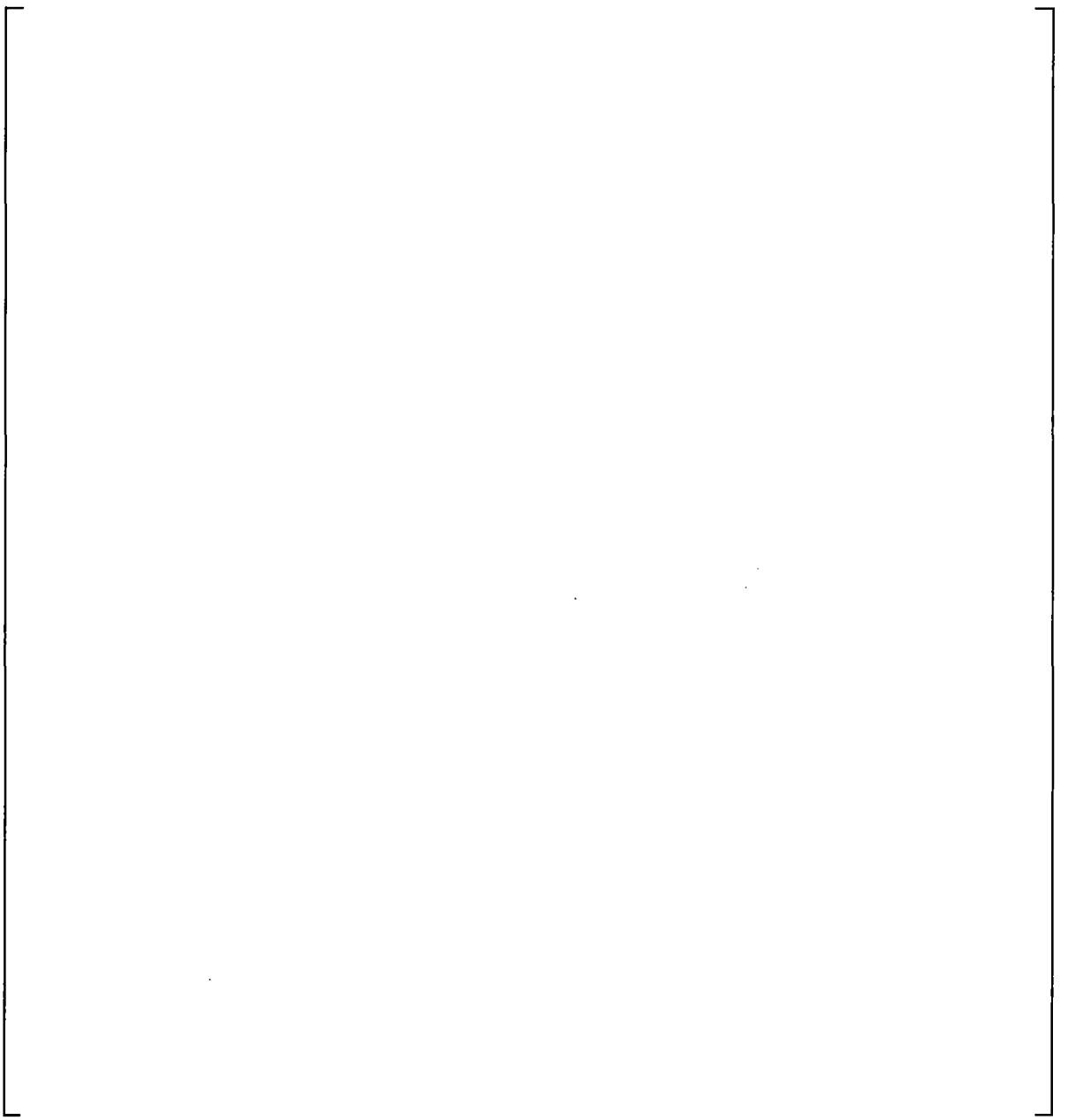

Figure 2-3 Geometry Plot: [ ]^{a,c}

a,c

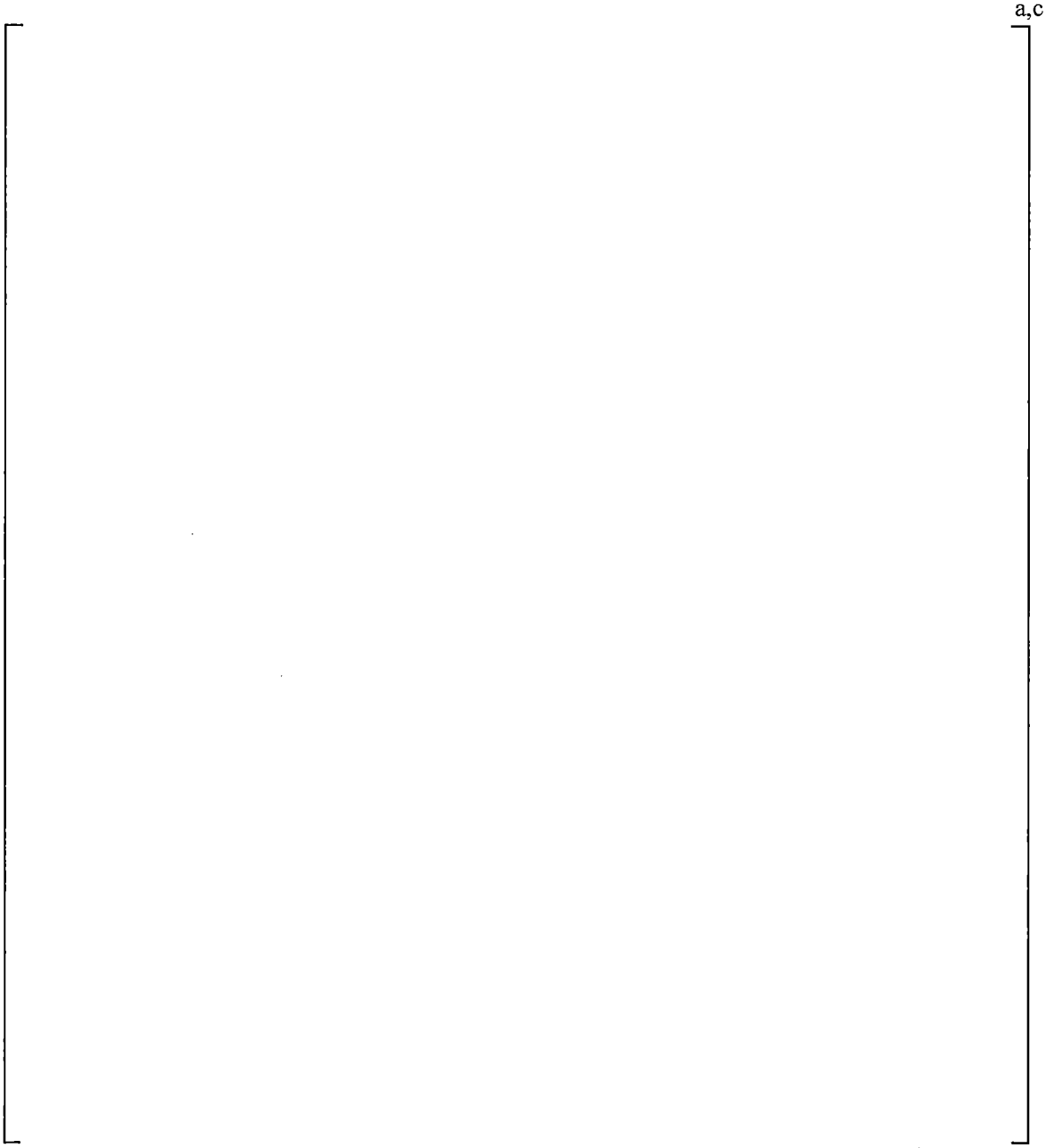

Figure 2-4 Geometry Plot: [ ]^{a,c}

a,c

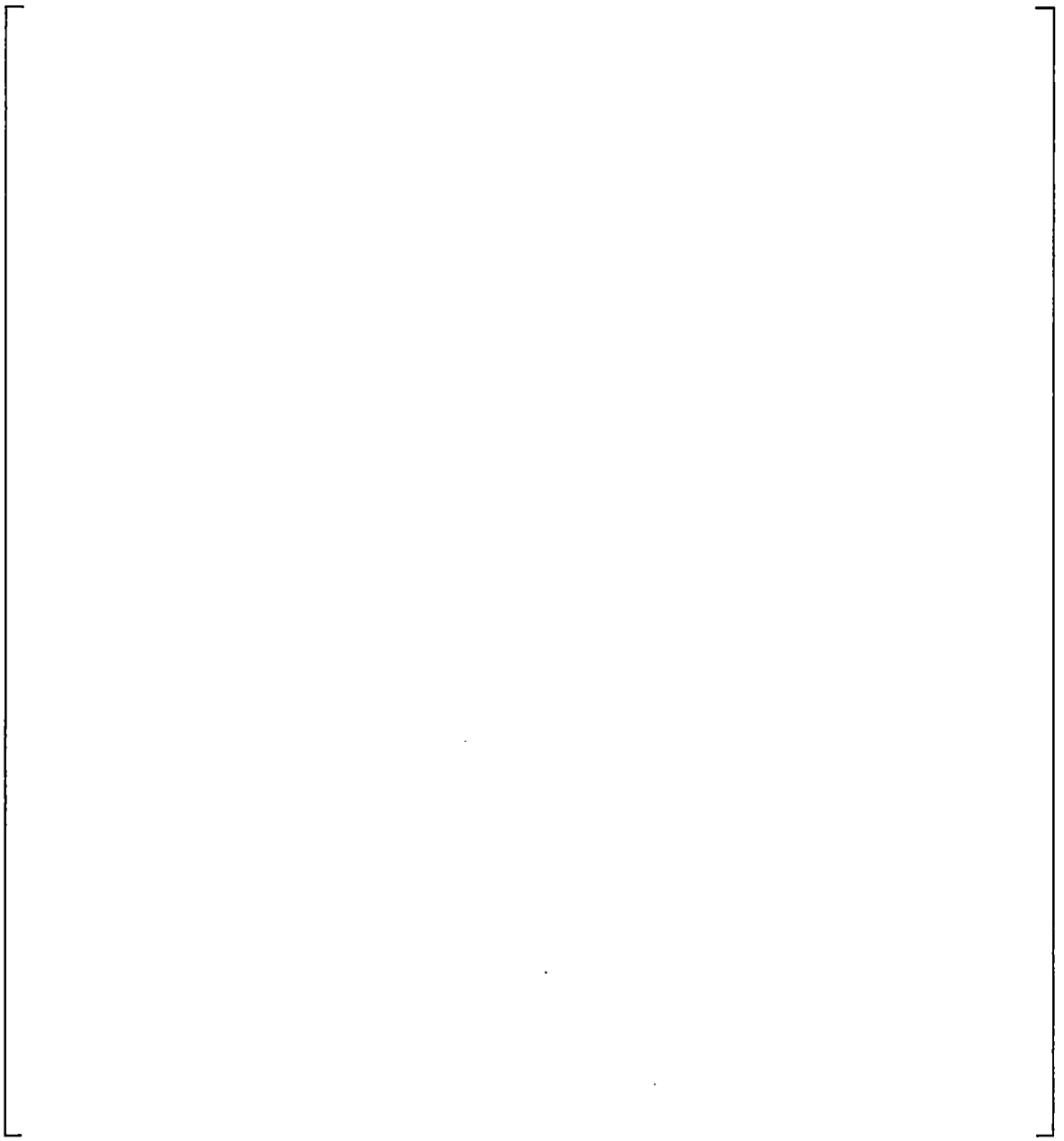

Figure 2-5 Geometry Plot: [ ]^{a,c}

a,c

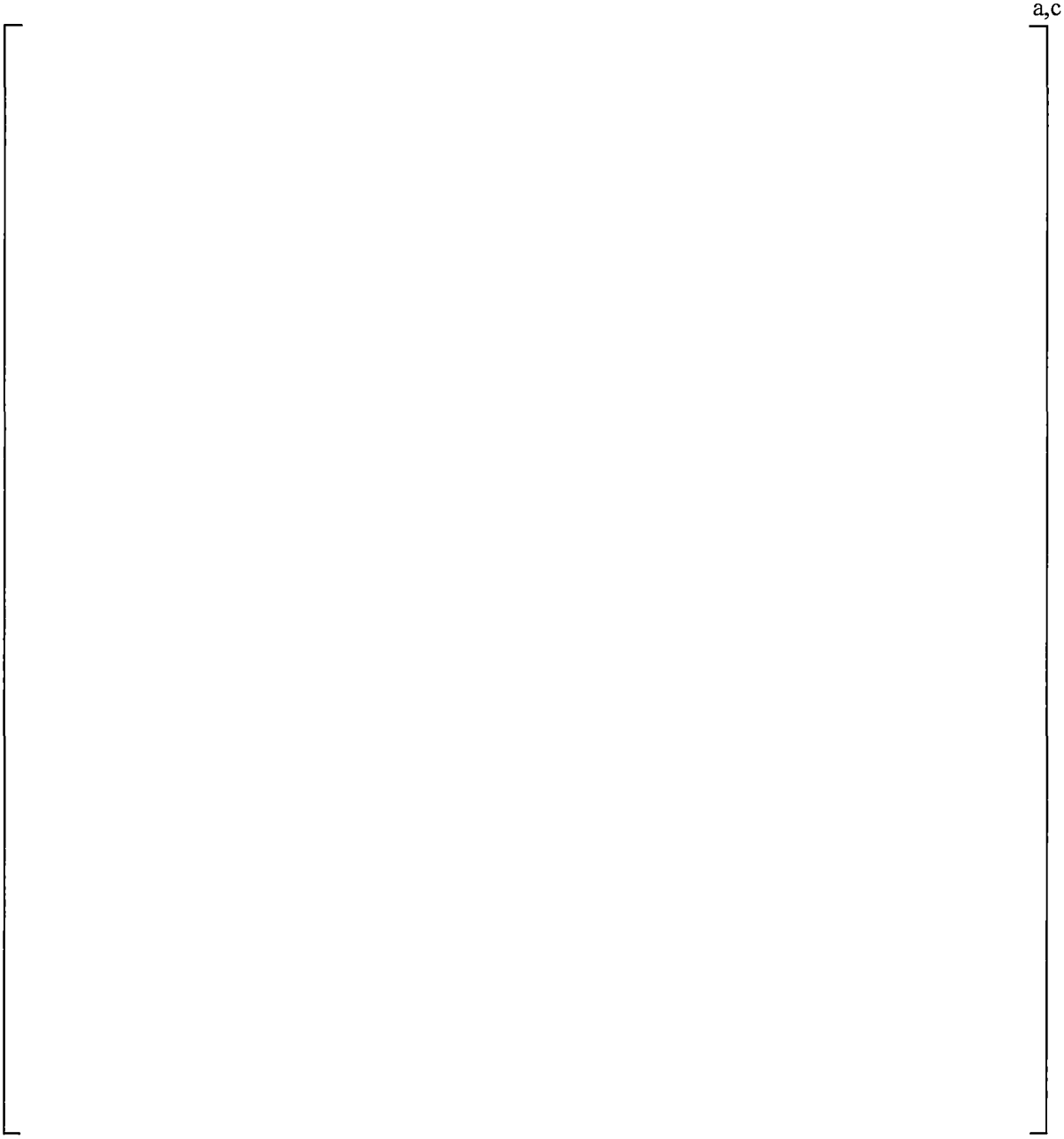

Figure 2-6 Geometry Plot: [ ]a,c

a,c

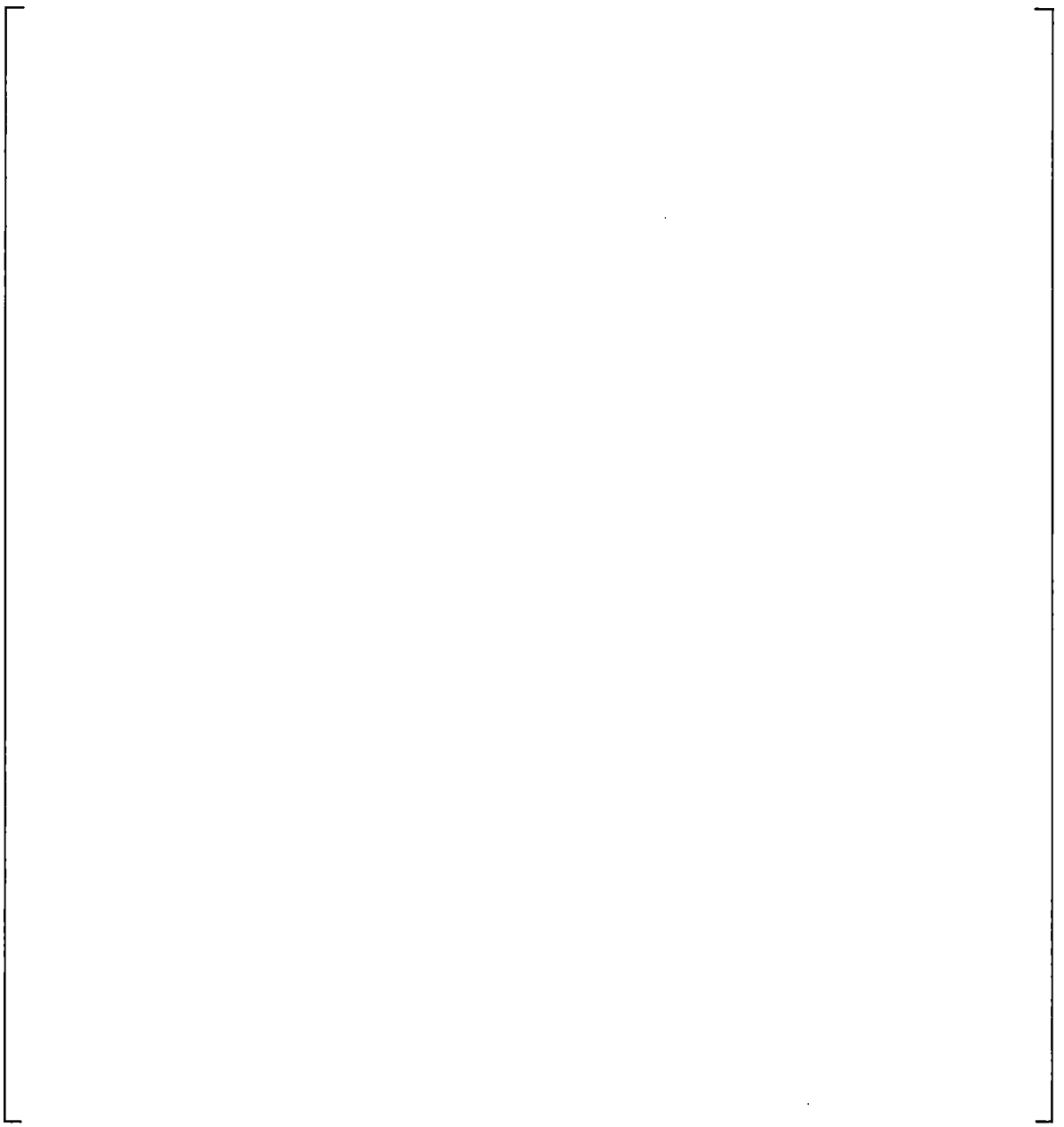

Figure 2-7 Geometry Plot: [ ]^{a,c}

3 FINITE ELEMENT MODEL DESCRIPTION

3.1 STEAM DRYER GEOMETRY

The Monticello replacement steam dryer FEM, generated using the ANSYS® computer code[1], is shown in Figure 3-1. The model consists primarily of [

]^{a,c}.

[

]^{a,c}.

The dryer structure includes [

]^{a,c}.

The [

]^{a,c}

[1] The analysis qualification of the Monticello replacement steam dryer was performed using the [
]^{a,c}

Figure 3-11 shows the [

]a,c

3.2 FINITE ELEMENT MODEL MESH AND CONNECTIVITY

The dryer plates are all modeled [

]a,c

The vane bank [

]a,c.

[

]a,c are shown in Figure 3-16.

3.2.1 Mesh Density Study

A mesh density study was performed using [

]a,c

3.2.2 Shell-Solid Connections in the FEM

A study was performed to investigate the load transfer between shells and solids using [

]^{a,c}

3.2.3 Vane Bank Representation

The vane bank modules are box-like structures with many internal hanging chevrons. [

]^{a,c} and are shown in more detail in Figure 3-17.

The perforated plates [

]^{a,c} are shown in Figure 3-18.

Also shown in Figure 3-18 are the [

]^{a,c}.

The vane bank [

]^{a,c} are shown in Figure 3-14.

3.2.4 Lifting Rod Representation

The lifting rod is modeled [

]^{a,c} are shown in Figure 3-16.

3.2.5 Beam – Solid Connections in the FEM

A study was performed to evaluate the moment transfer and adequacy of the [

]^{a,c}

3.2.6 Dryer Skirt Submerged in Water

The dryer skirt is partially submerged in water. [

]^{a,c}

a,c

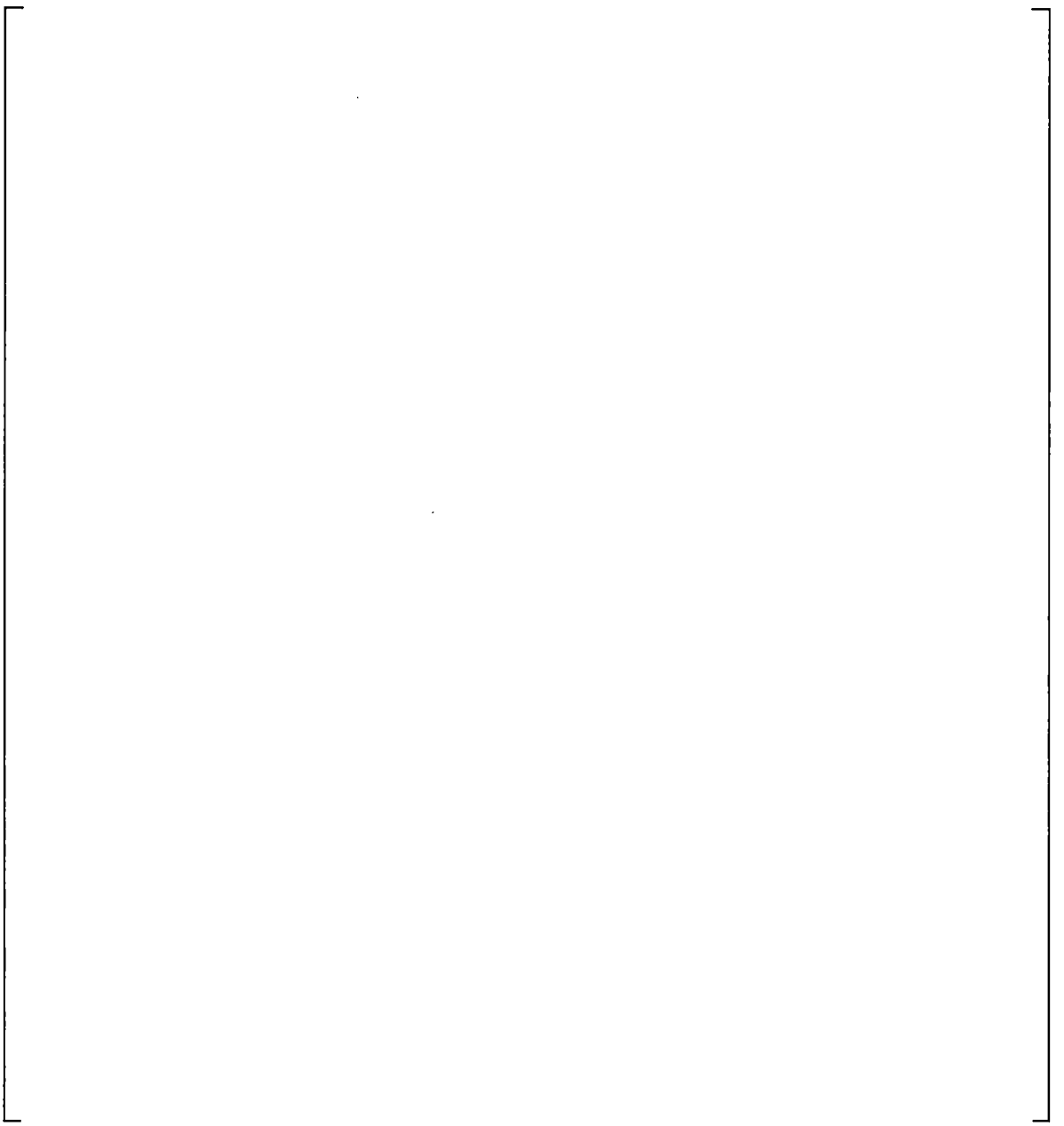

Figure 3-1 Monticello Replacement Steam Dryer Finite Element Model

a,c

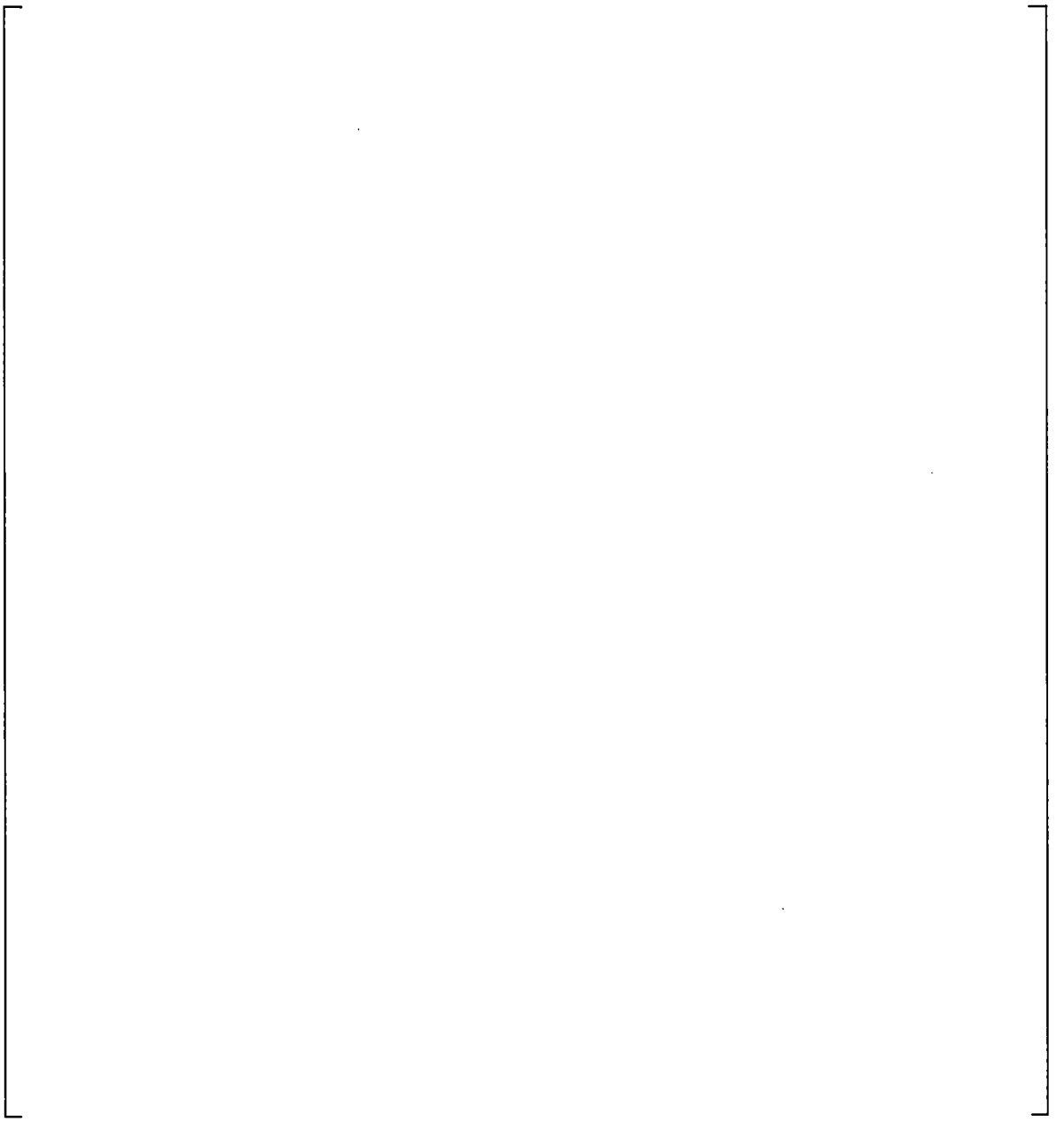

Figure 3-2 Lower [ ]^{a,c}

a,c

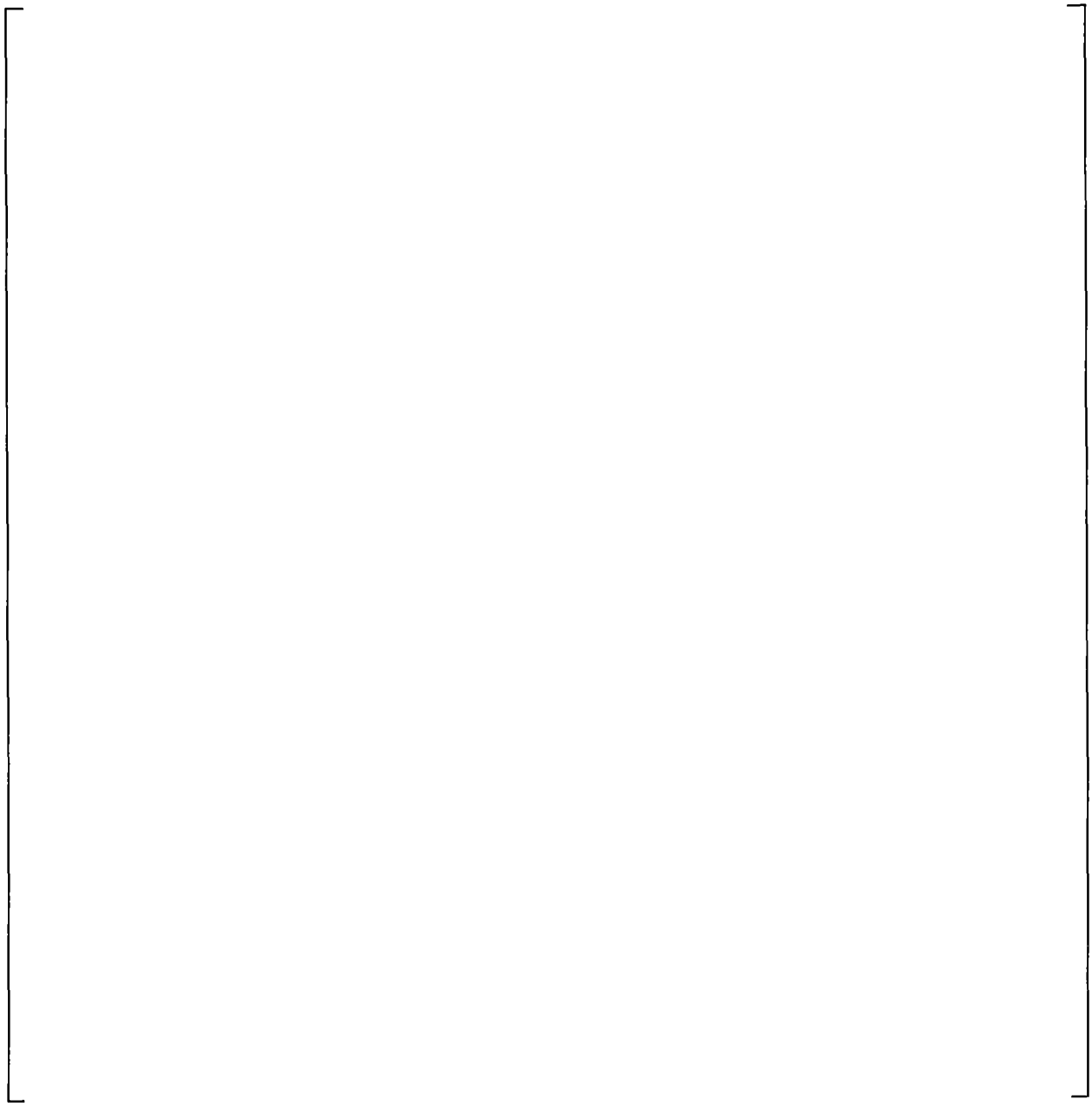

Figure 3-3 Lower [ ]^{a,c}

a,c

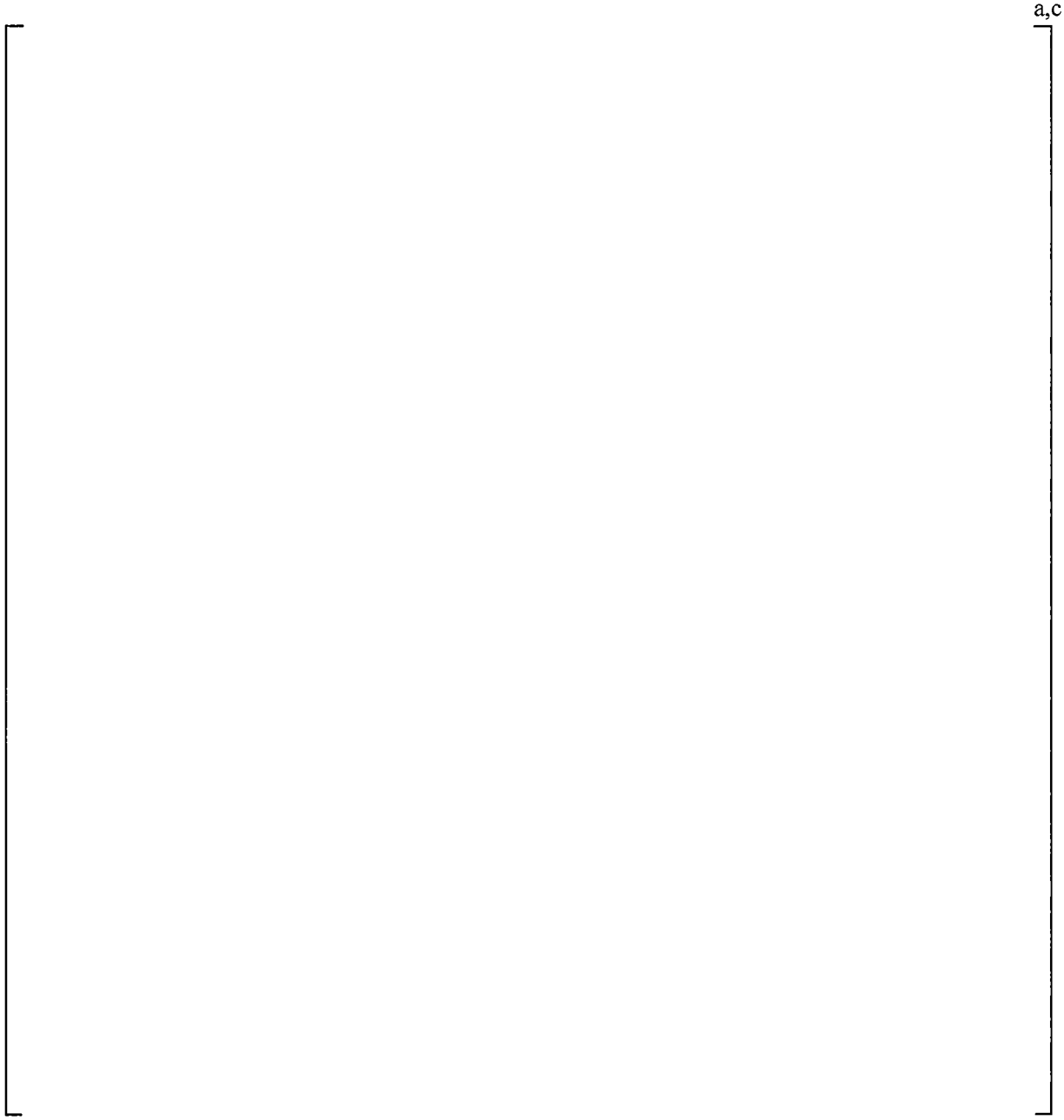

Figure 3-4 Vane Bank Structural Components

a,c

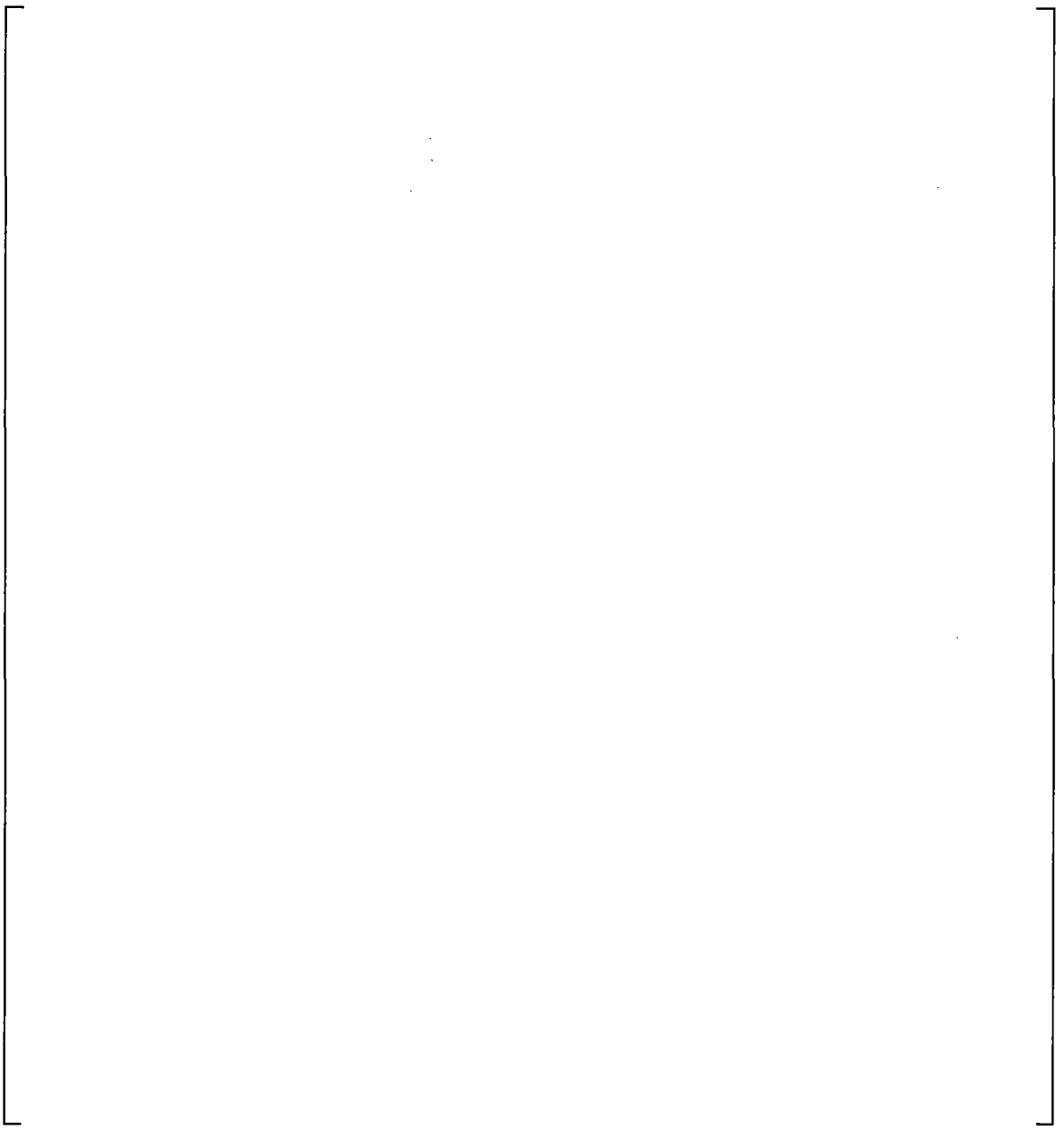

Figure 3-5 Vane Bank Geometry

a,c

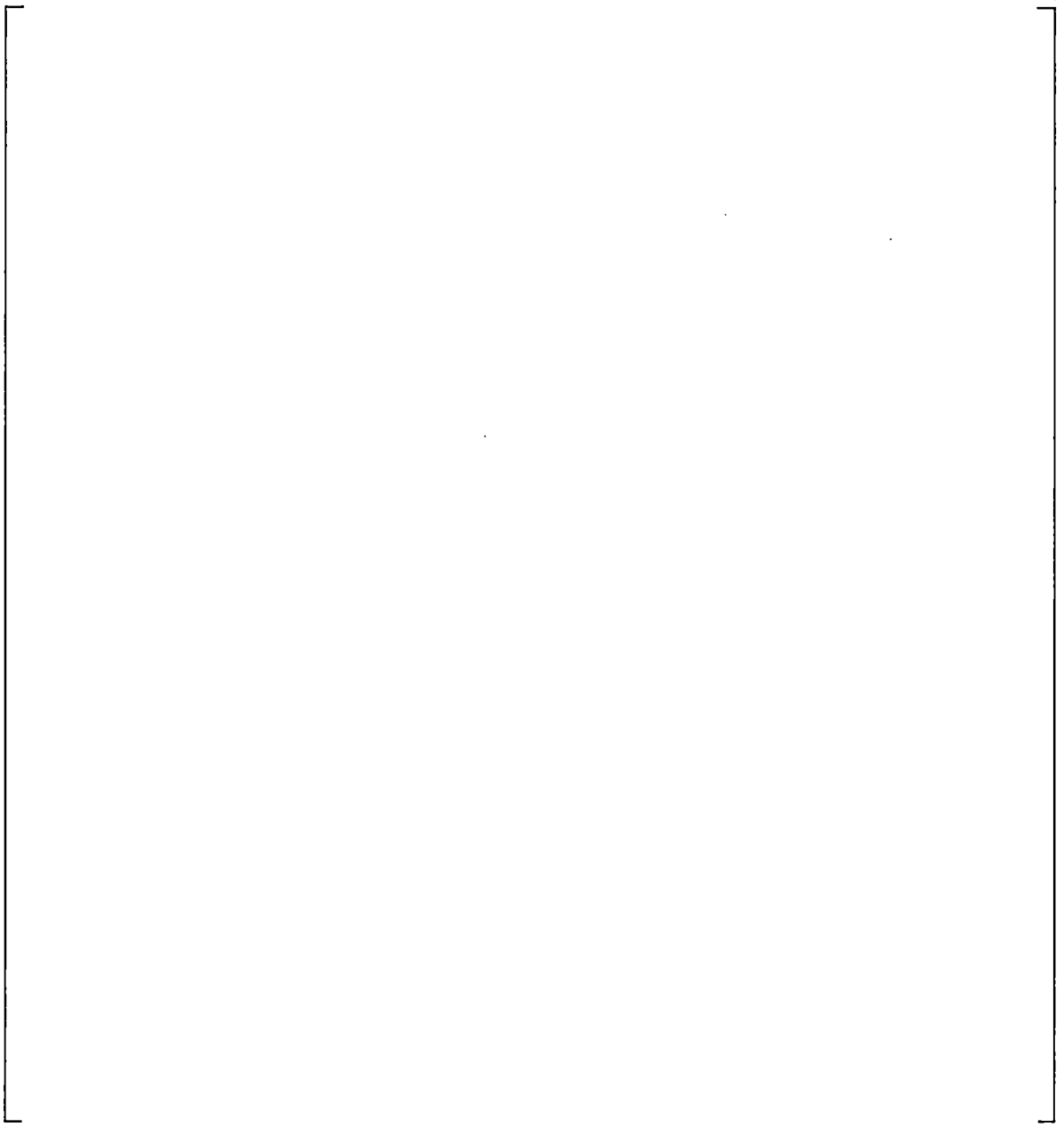

Figure 3-6 Dryer Hood Geometry

a,c

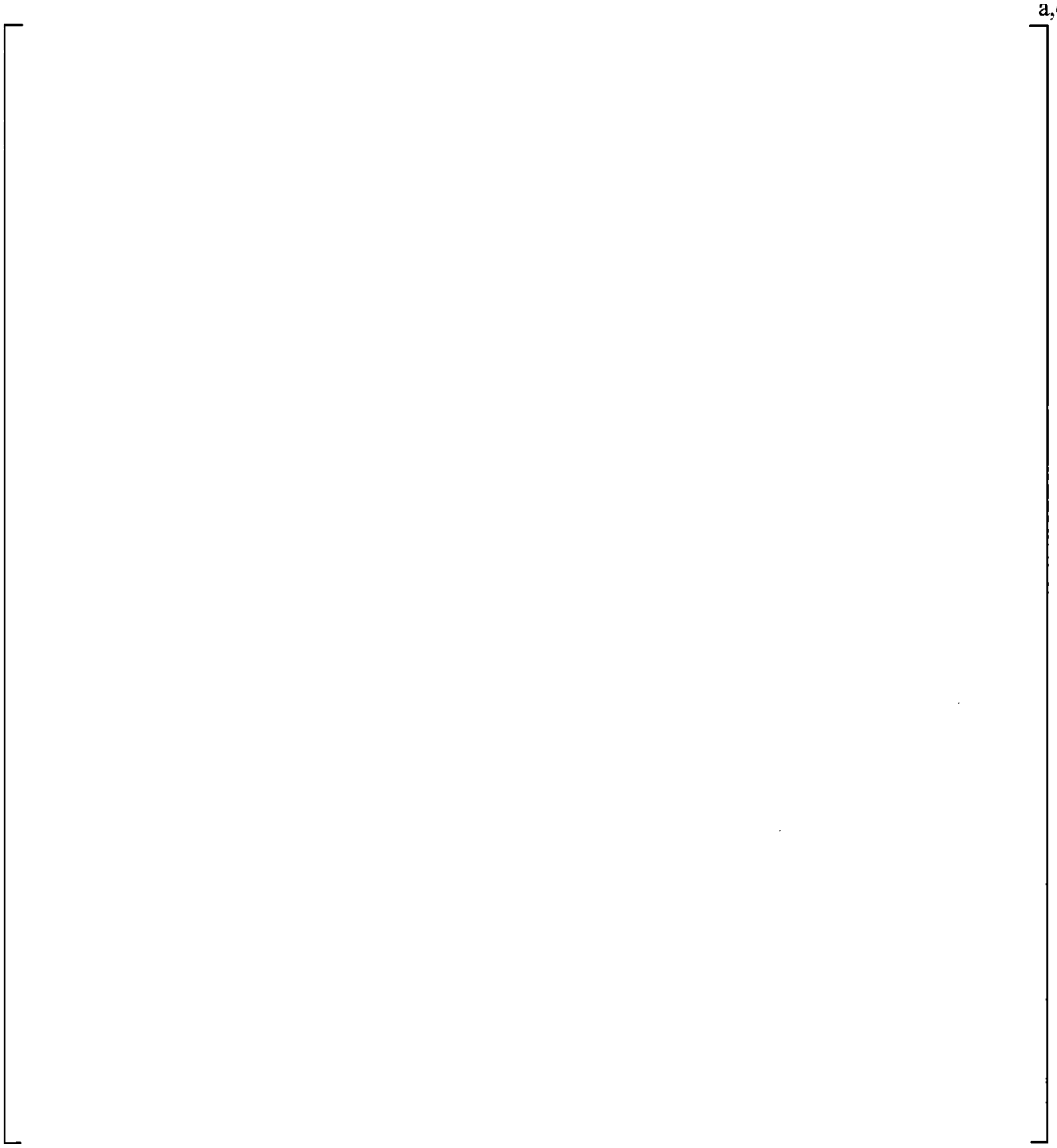

Figure 3-7 Skirt Geometry

a,c

[ ]

Figure 3-8 [ ][a,c]

a,c

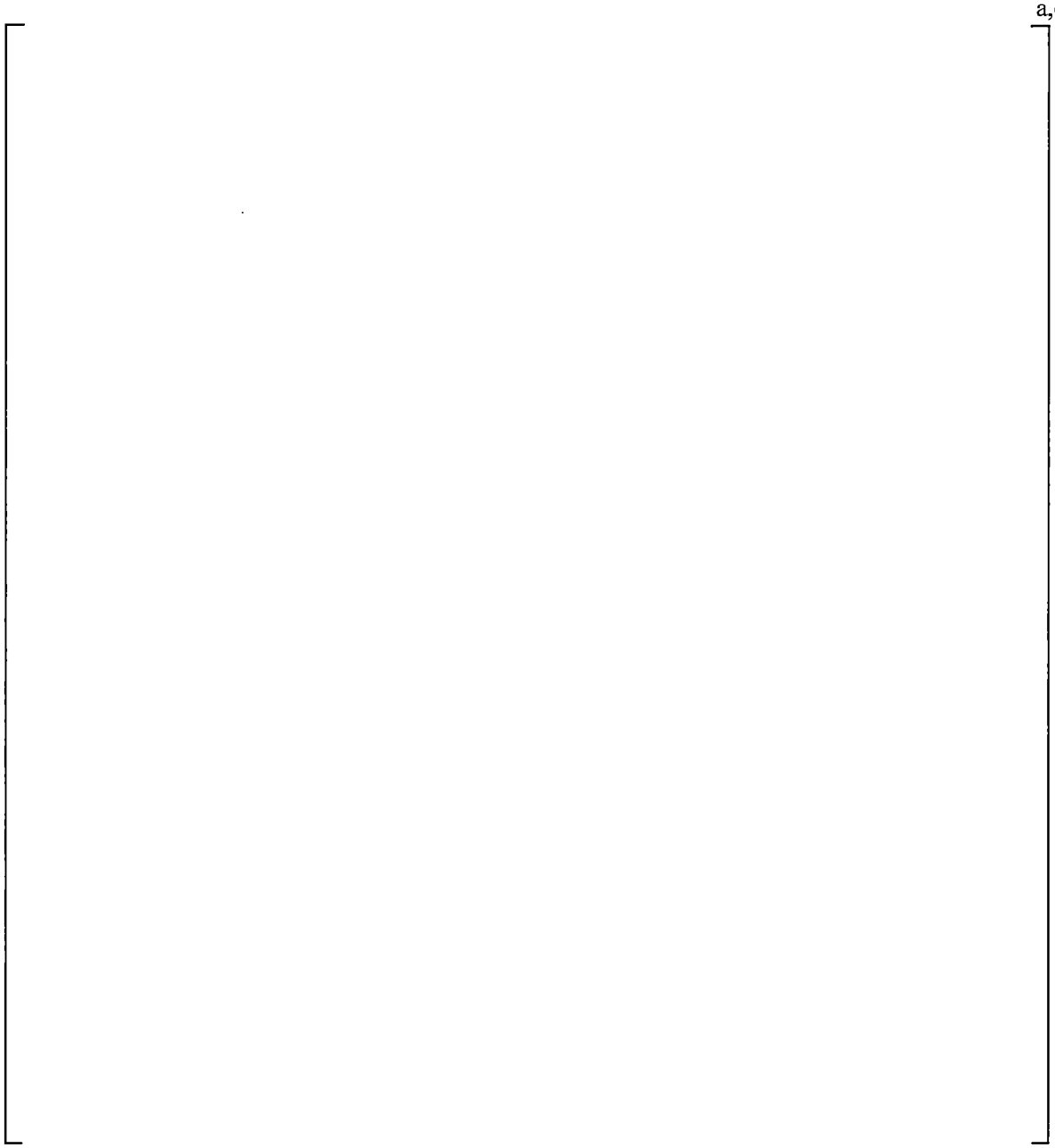

Figure 3-9 [ ][a, c]

a,c

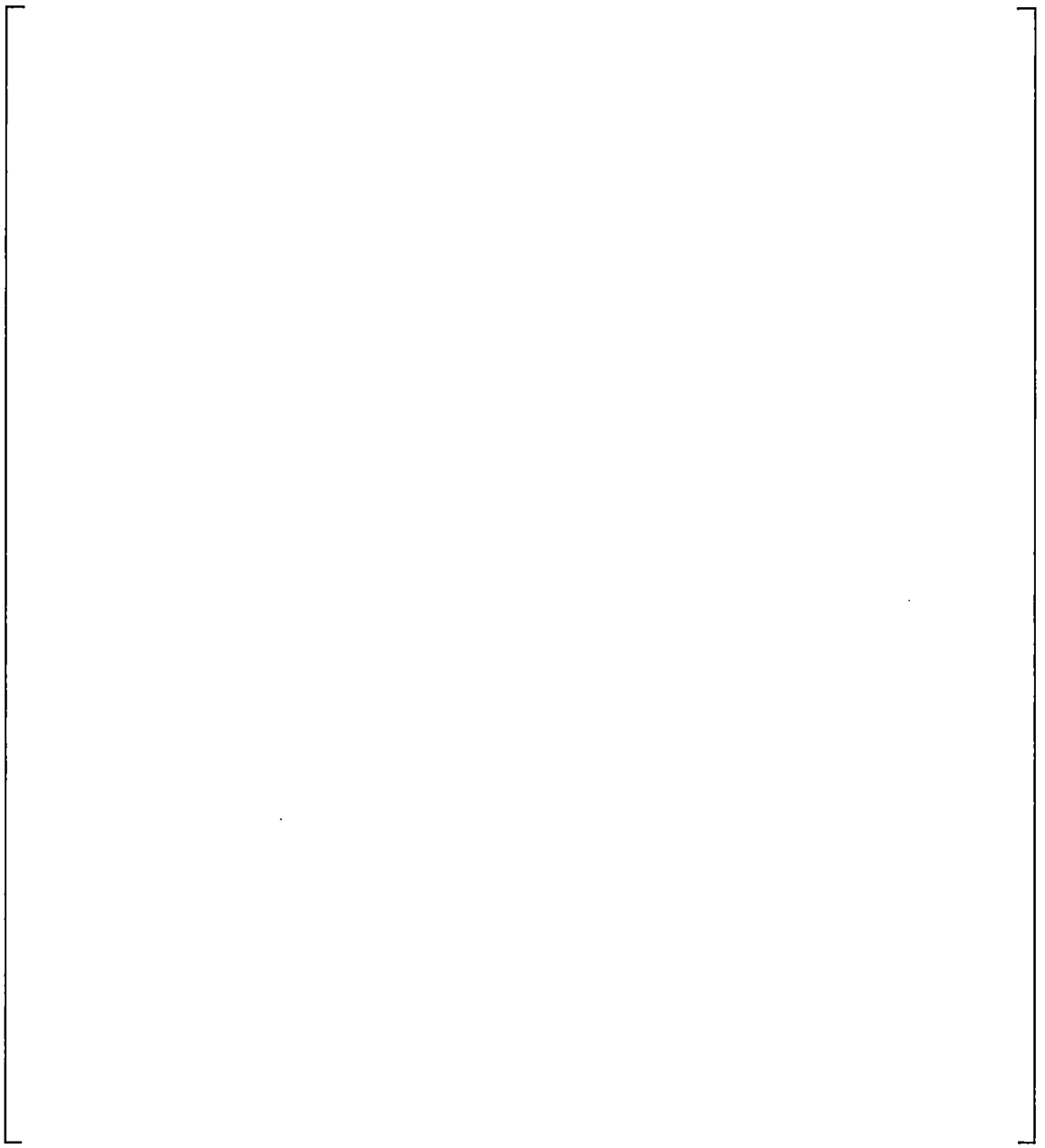

Figure 3-10 [ ][a,c]

a,c

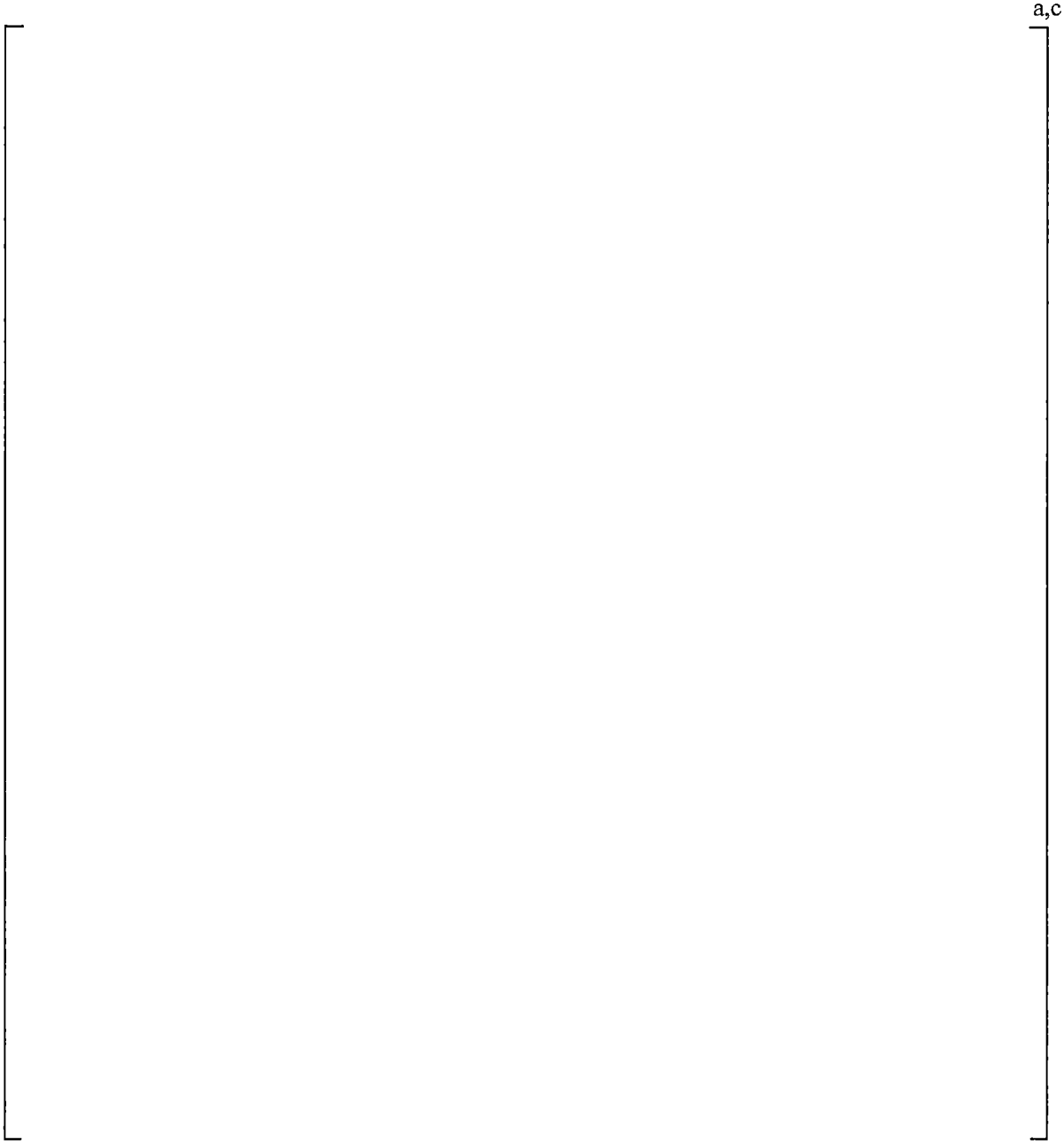

Figure 3-11 Lifting Rod Geometry

a,c

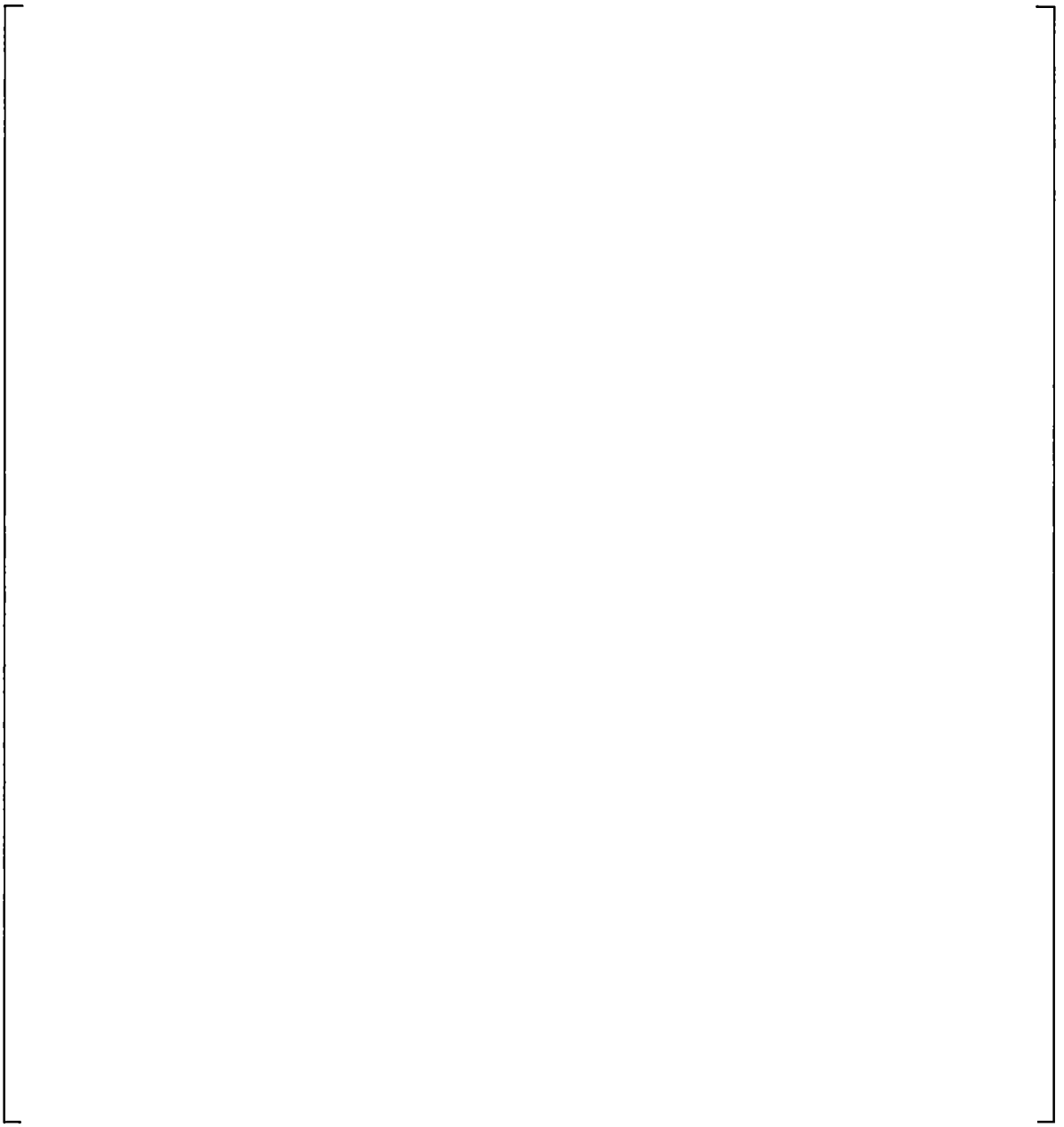

Figure 3-12 [ ][a, c]

a,c

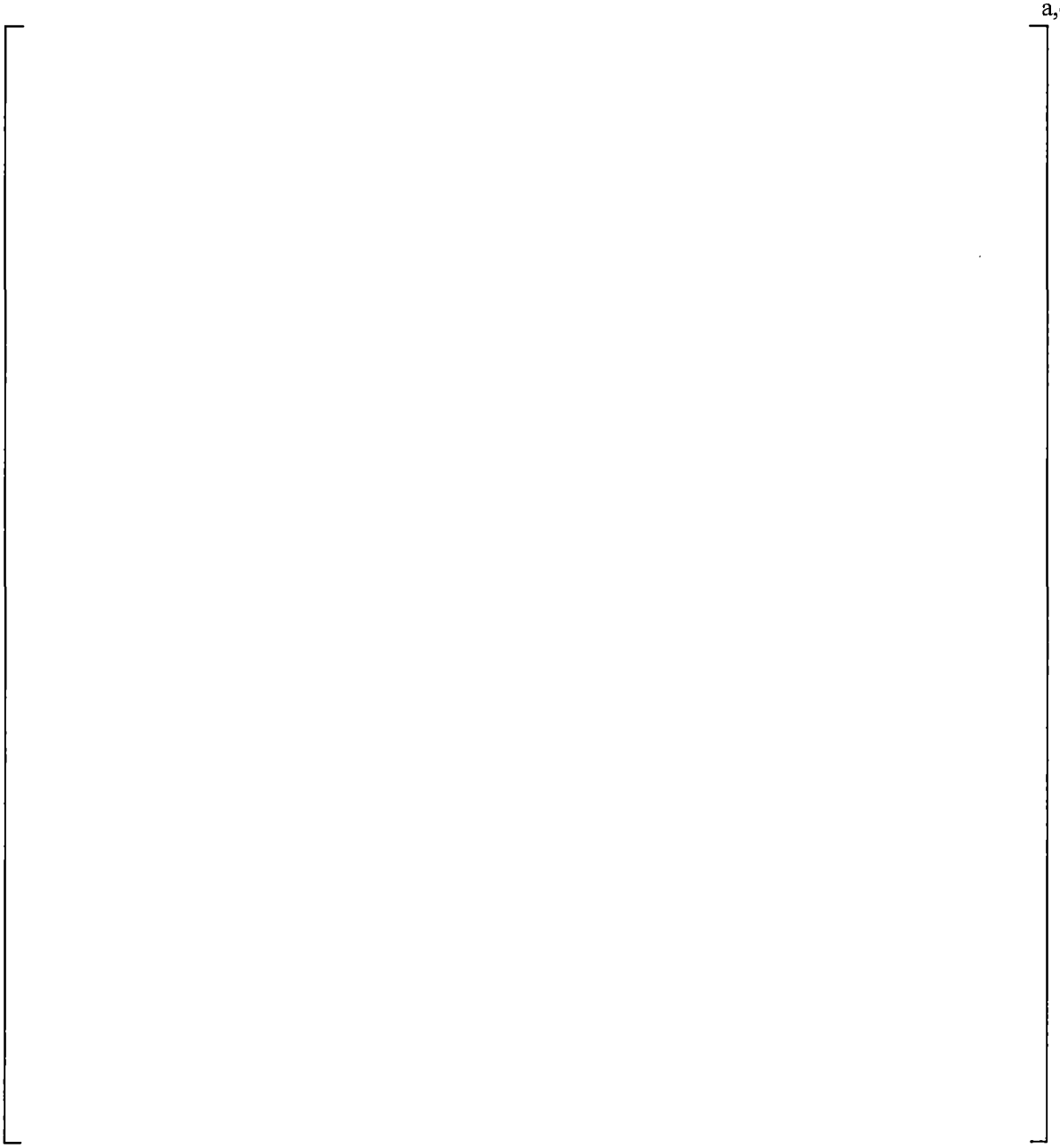

Figure 3-13 [ ][a,c]

a,c

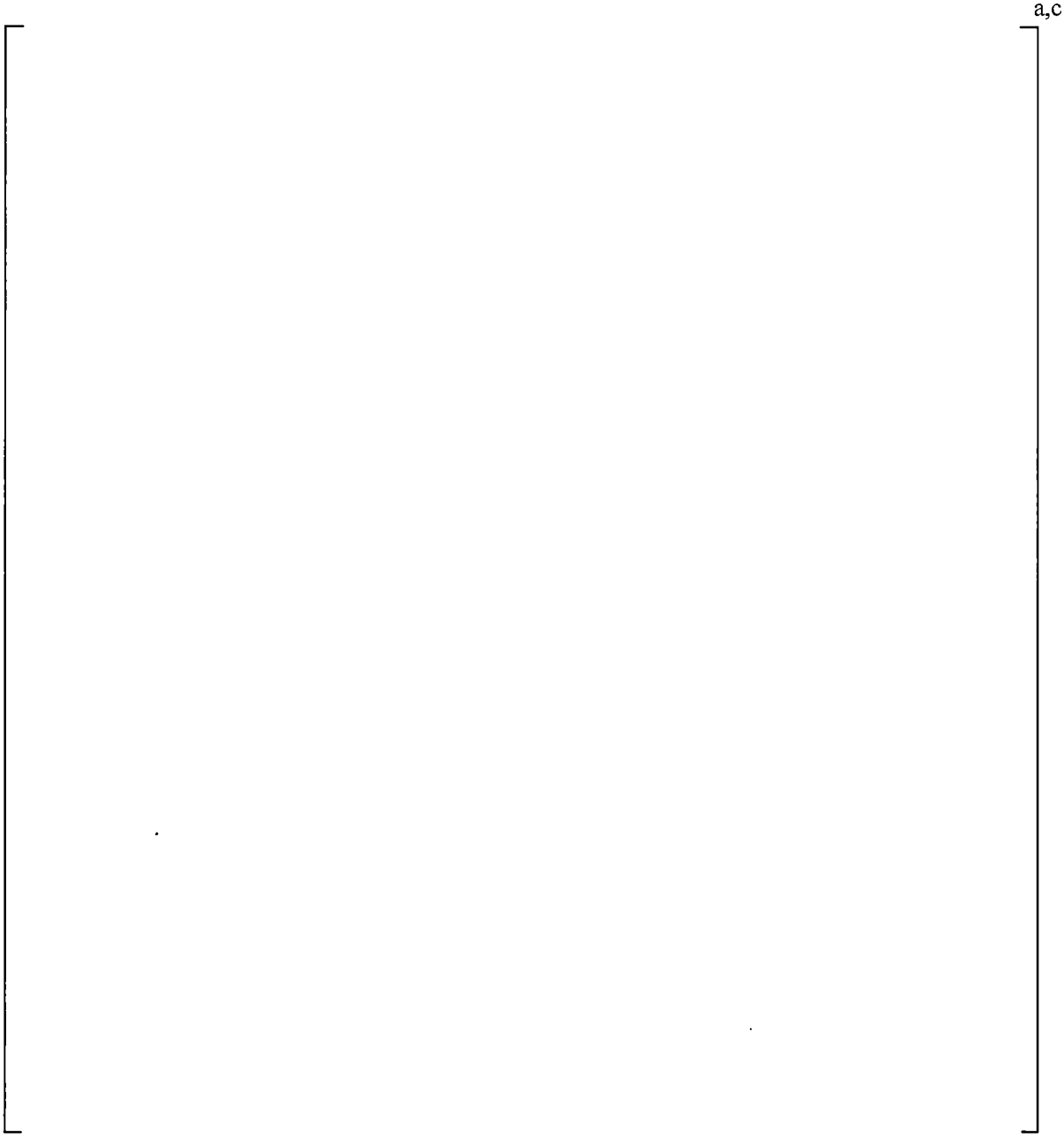

Figure 3-14 [**]**[a, c]**

a,c

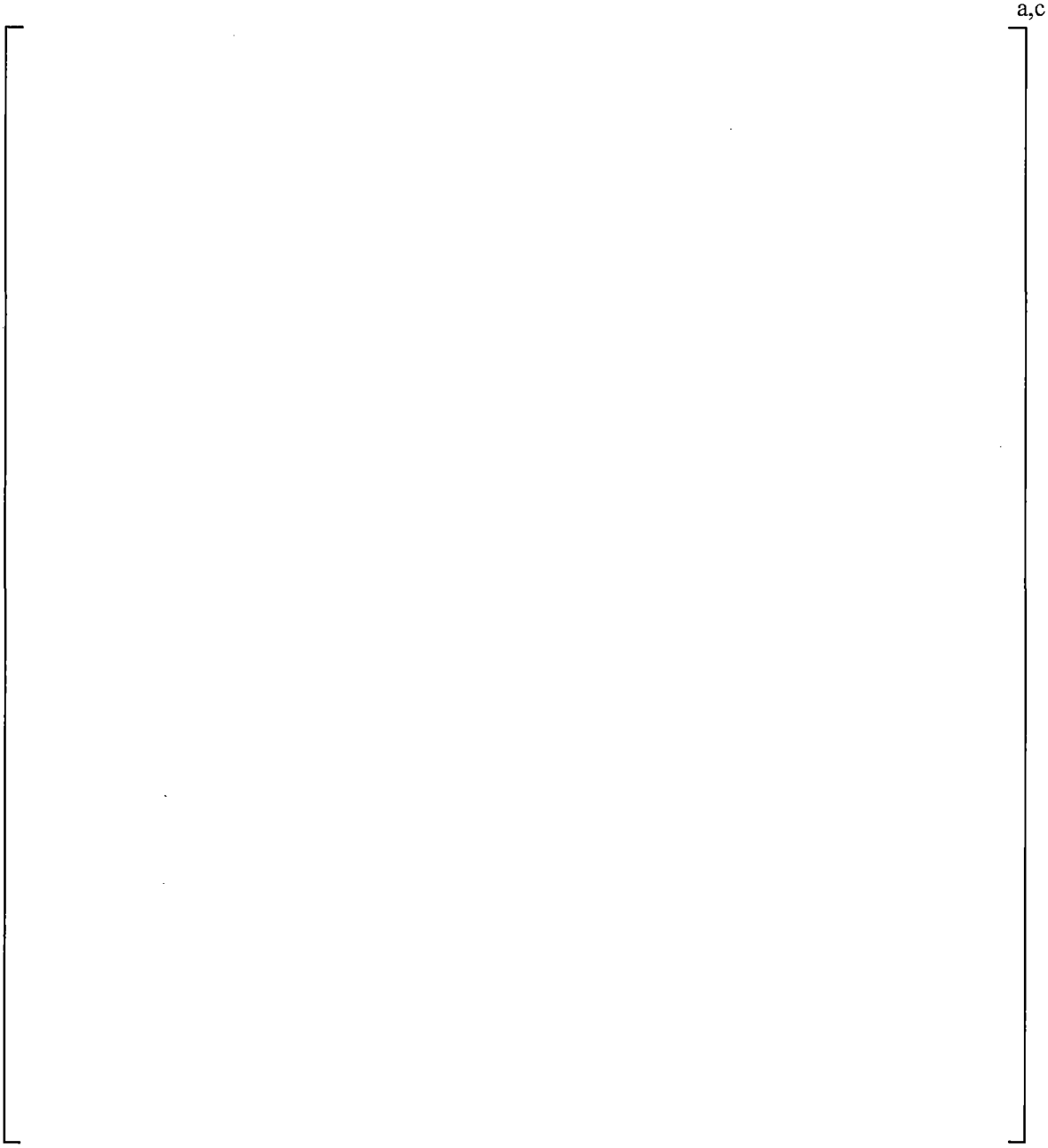

Figure 3-15 [ ][a,c]

a,c

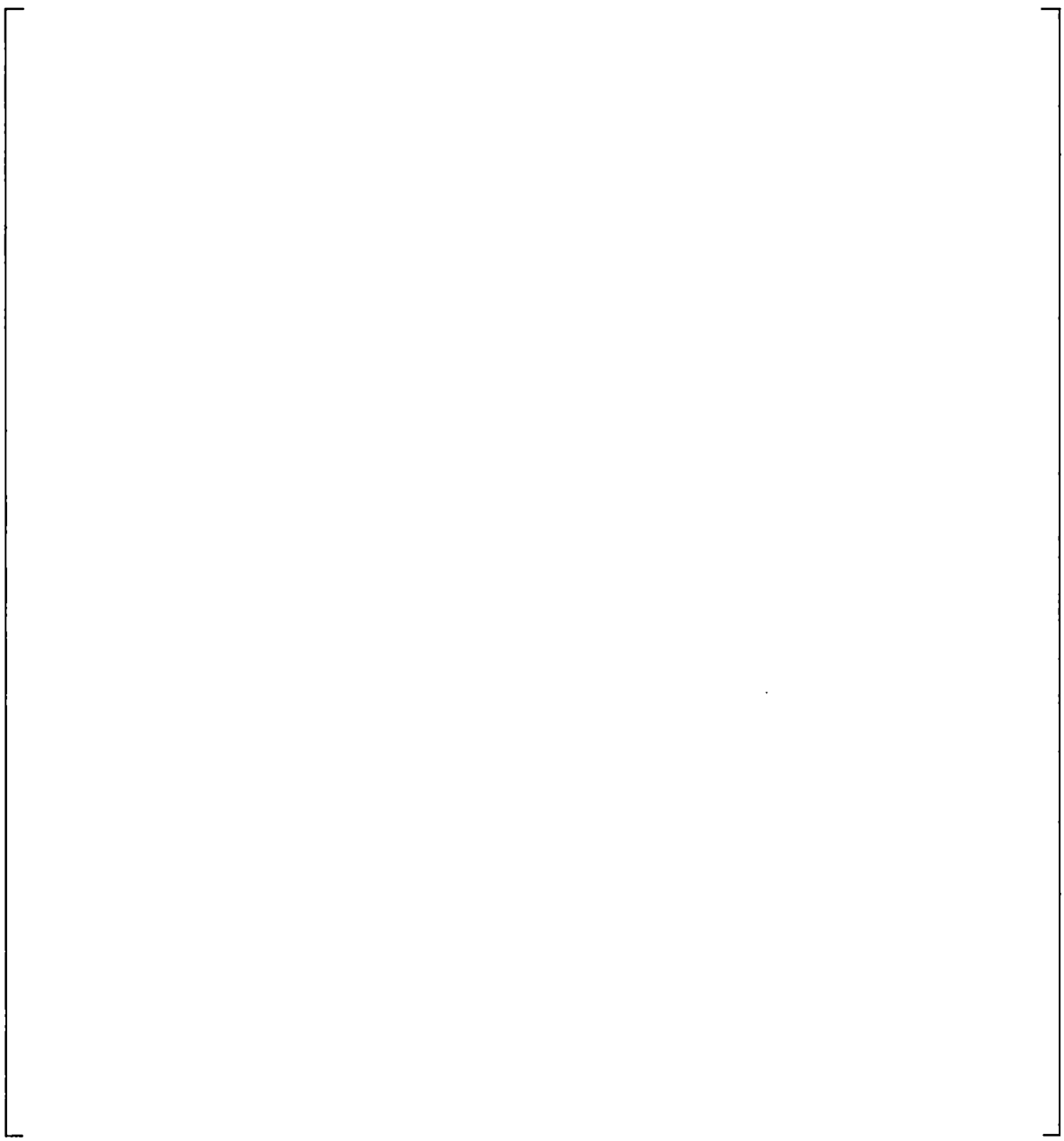

Figure 3-16 [ ][a,c]

a,c

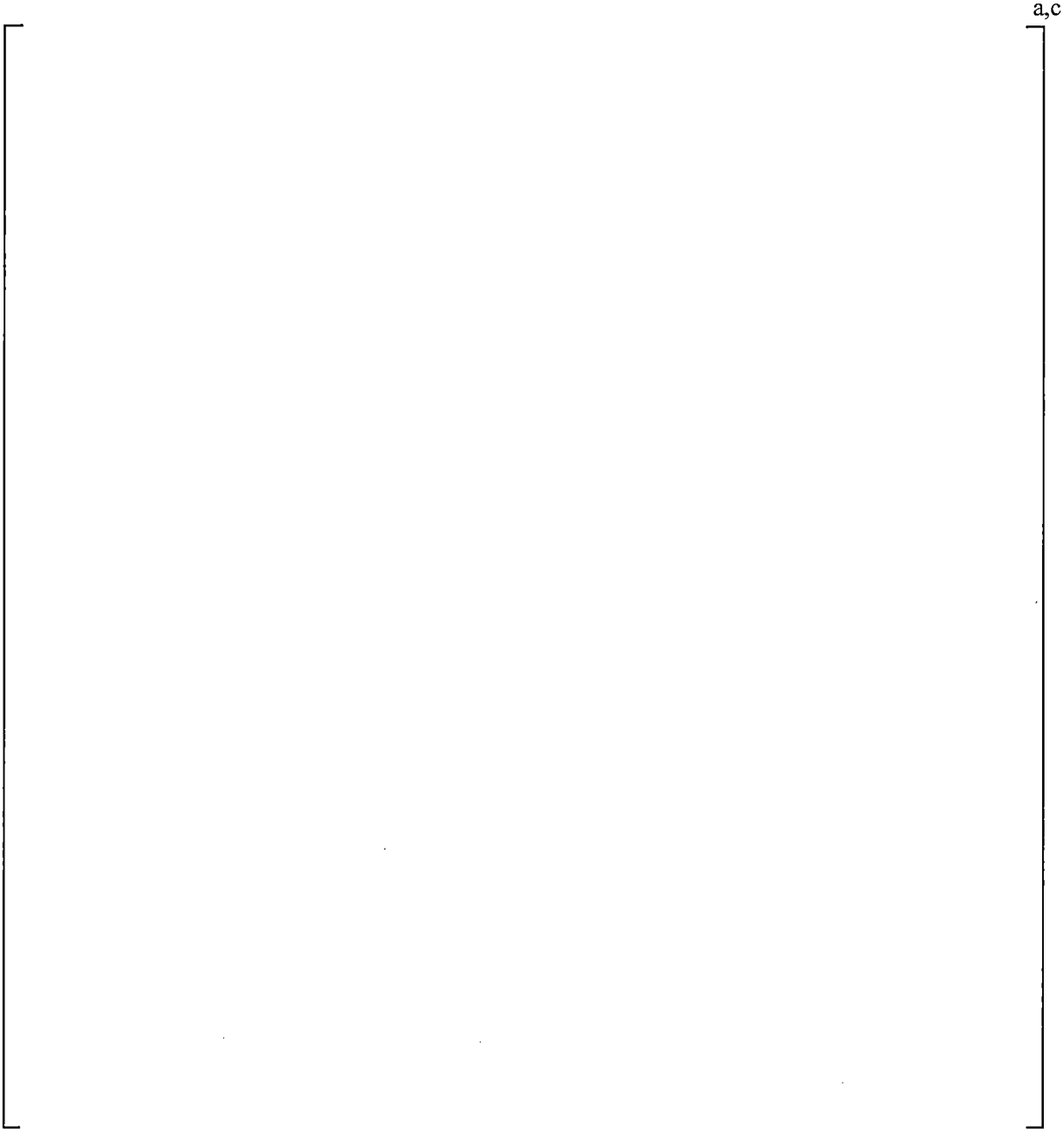

Figure 3-17 Structural Components of Vane Bank

a,c

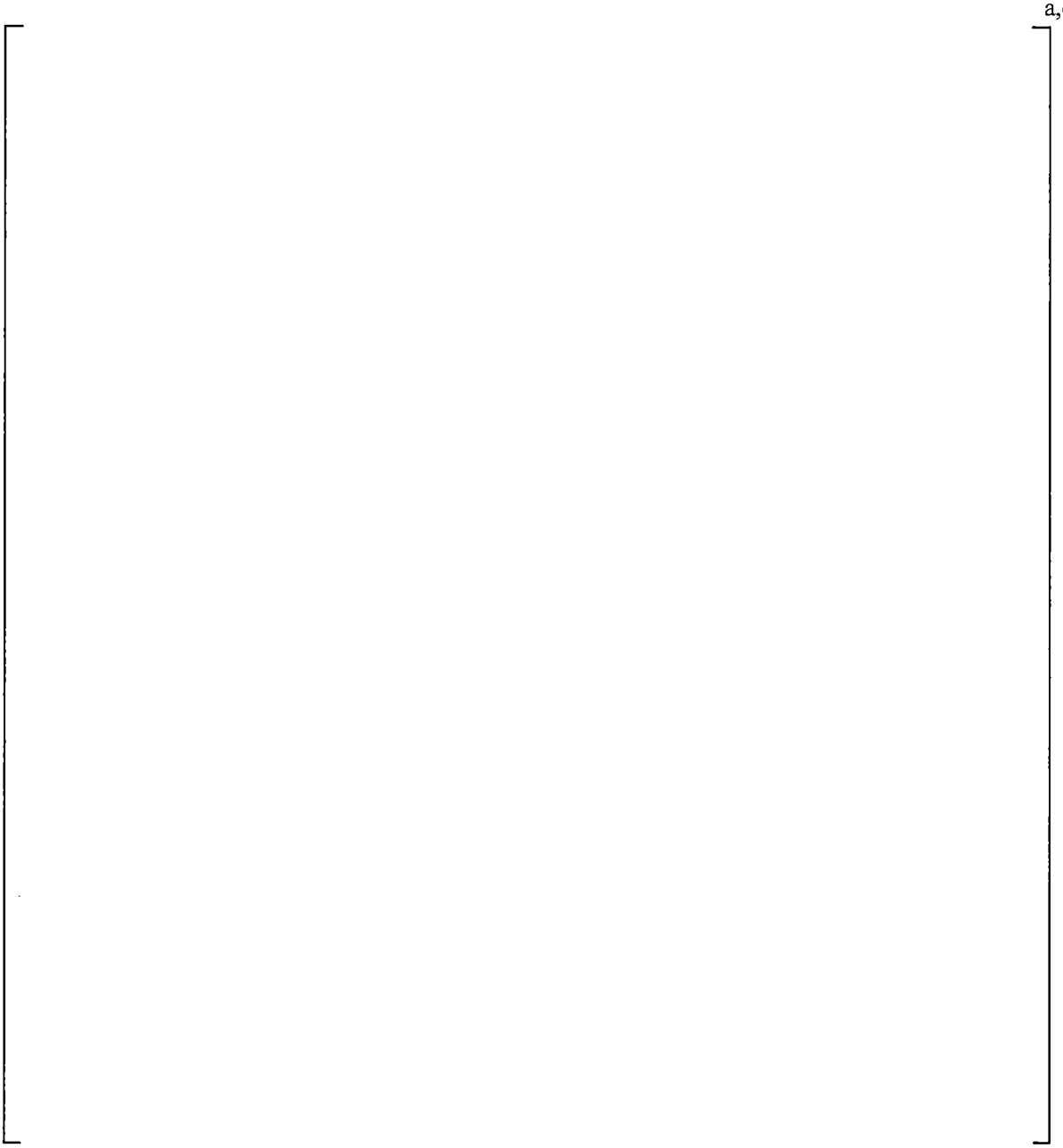

Figure 3-18 Structural and Non-Structural Components of Vane Bank

a,c

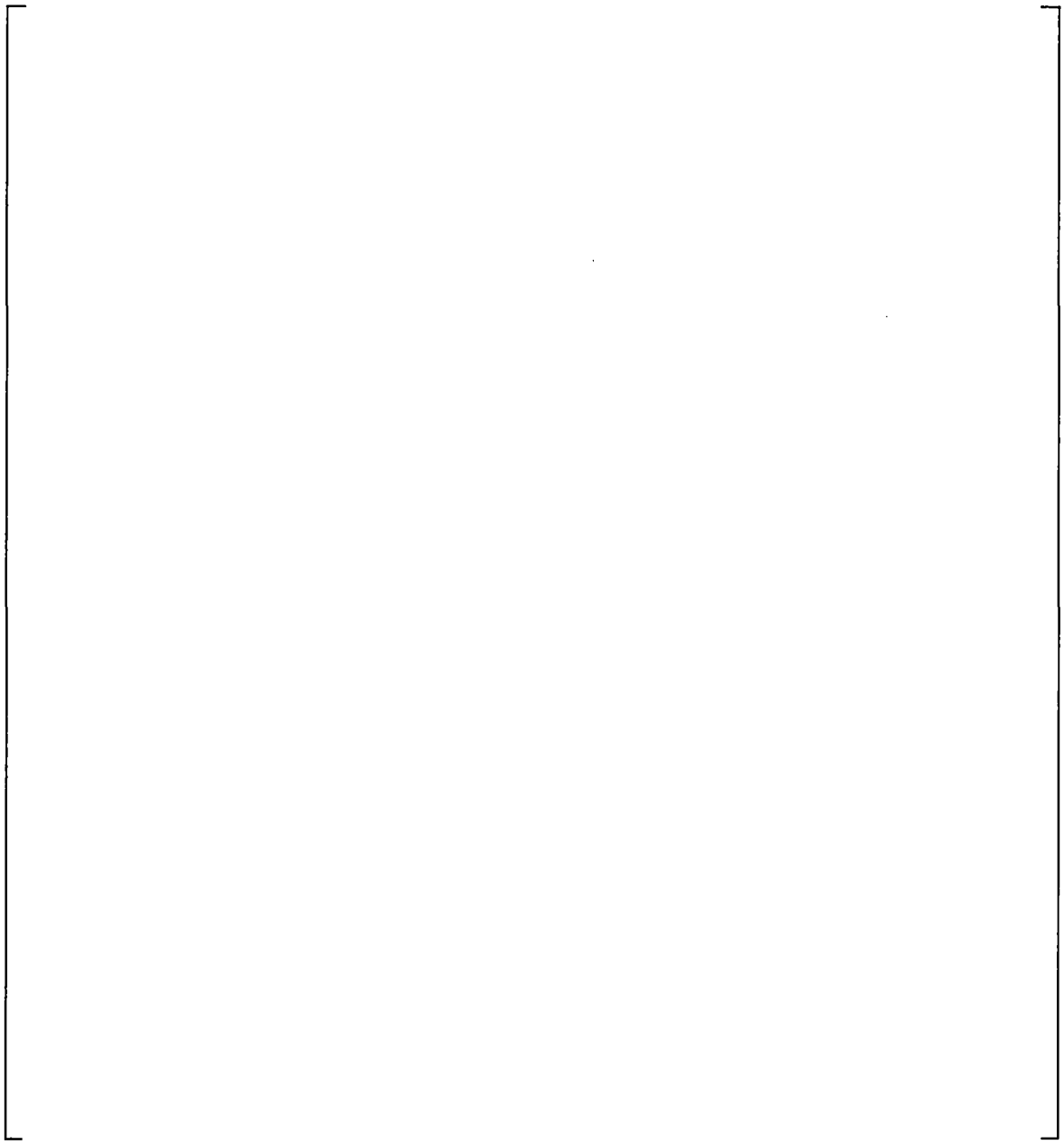

Figure 3-19 Vane Bank Mass Blocks

a,c

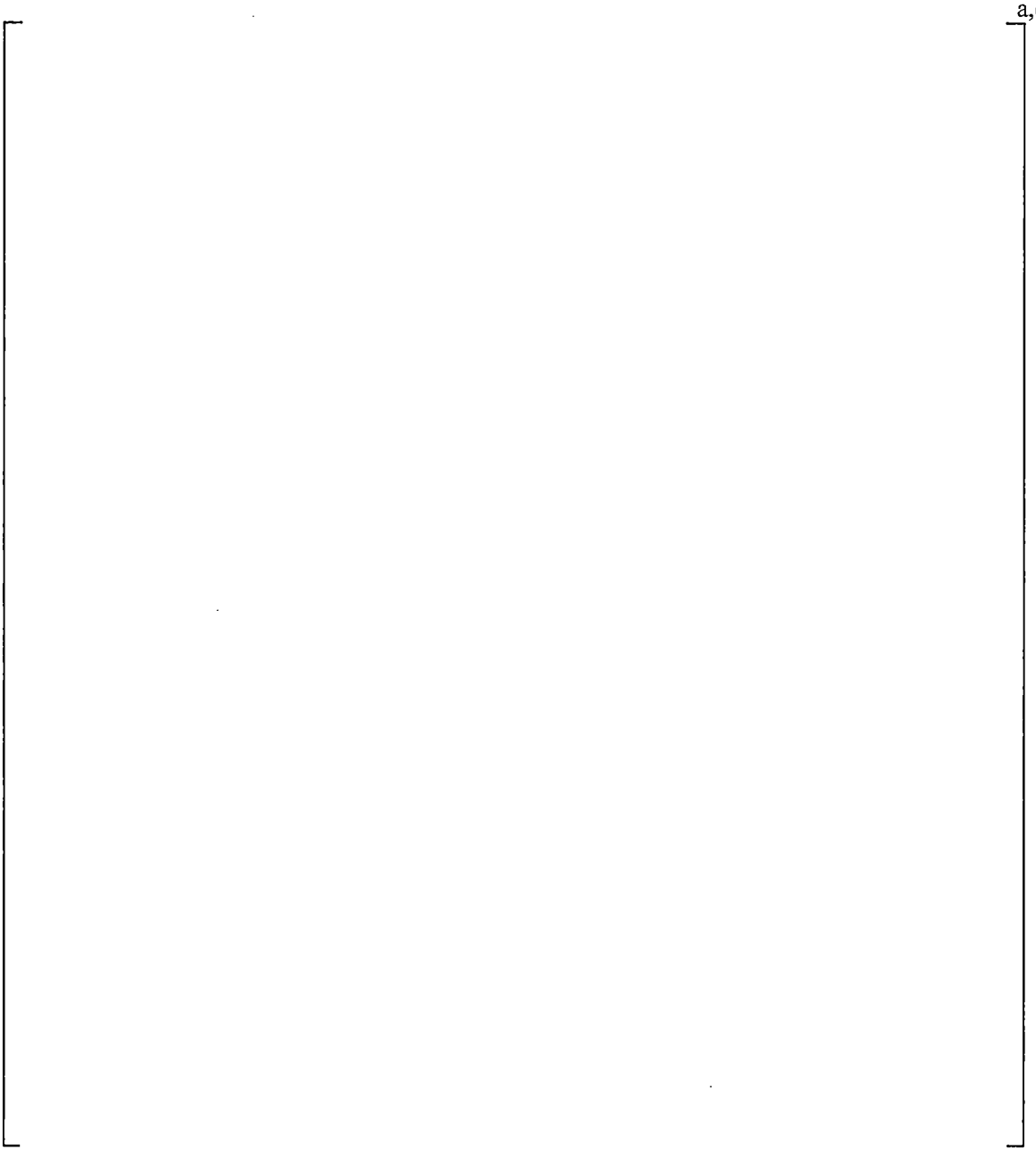

Figure 3-20 [ ][a,c]

4 MATERIAL PROPERTIES

The material properties used in the structural analysis are summarized in Table 4-1. Material properties are taken from the ASME Code, Reference 2, for [

]^{a,c} are summarized in Table 4-2.

4.1 STRUCTURAL DAMPING

Structural damping is defined as 1% of critical damping for all frequencies. This damping is consistent with guidance given on page 10 of NRC RG-1.20 (Reference 3). Using the harmonic analysis approach, a consistent damping level is used across the frequency domain.

Table 4-1 Summary of Material Properties a,b,c

Table 4-2 Summary of Vane Bank [ ]^{a,b,c} a,b,c

5 MODAL ANALYSIS

As a precursor to performing the transient analysis, a modal analysis of the dryer was performed. The modal analysis was performed for modes between 0 Hz and 140 Hz. Some modes for the hood and skirt are shown in Figure 5-1 through Figure 5-4. The fundamental modes for the [

]^{a,c}, respectively. The acoustic fatigue evaluation includes loads in the range from 0 Hz to 250 Hz. This modal analysis is not intended to be complete but only a check of the finite element model.

a,c

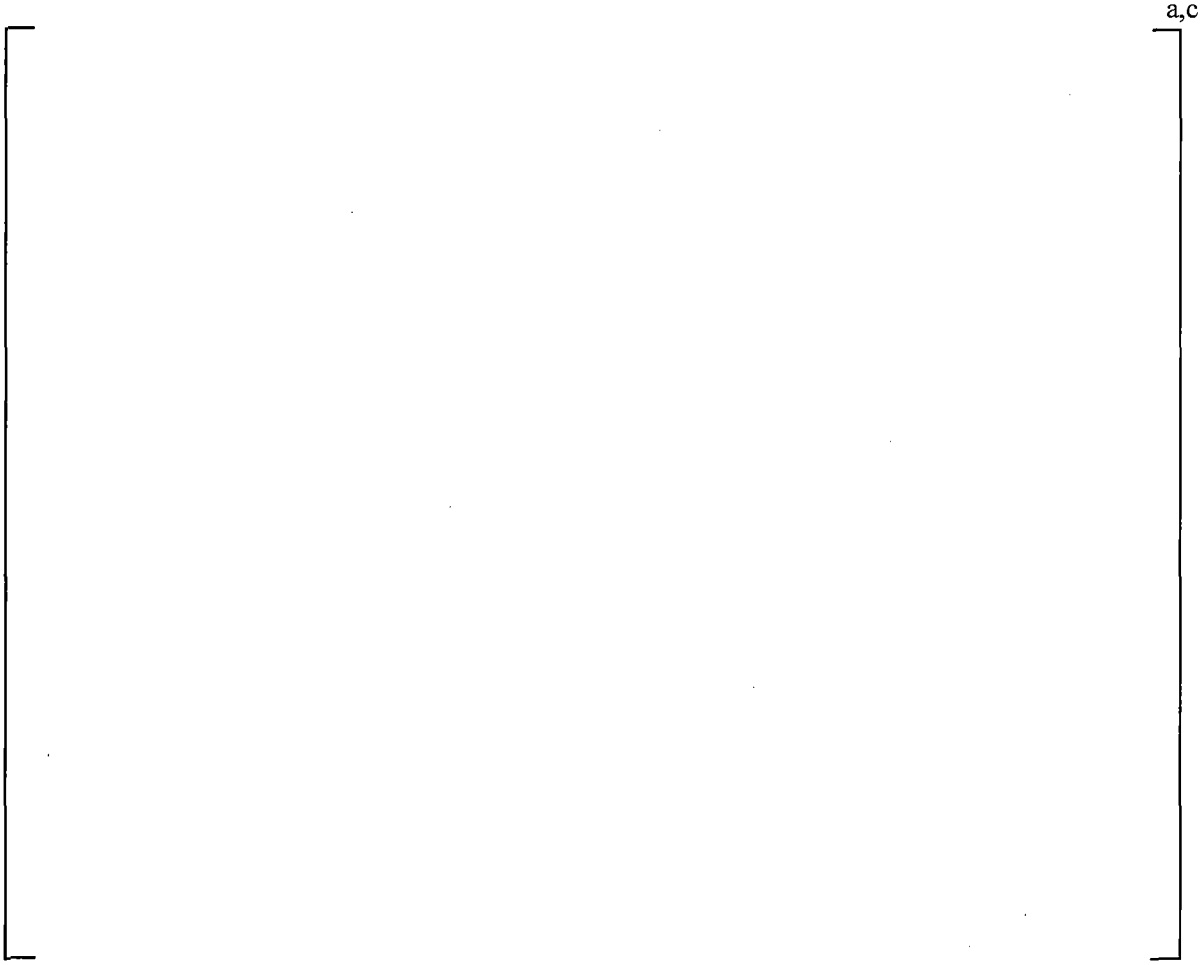

Figure 5-1 Modal Analysis: [ ]a,c

a,c

Figure 5-2 Modal Analysis: [ ]^{a,c}

a,c

Figure 5-3 Modal Analysis: [ ][a,c]

a,c

Figure 5-4 Modal Analysis: [ ]^{a,c}

6 LOAD APPLICATION

The frequency-dependent acoustic loads were developed using a three-dimensional (3-D) acoustic model representation of the dryer assembly. The acoustic pressure (P) loads on the steam dryer structure were calculated by [

]^{a,c}

[

]a,c

[a,b,c

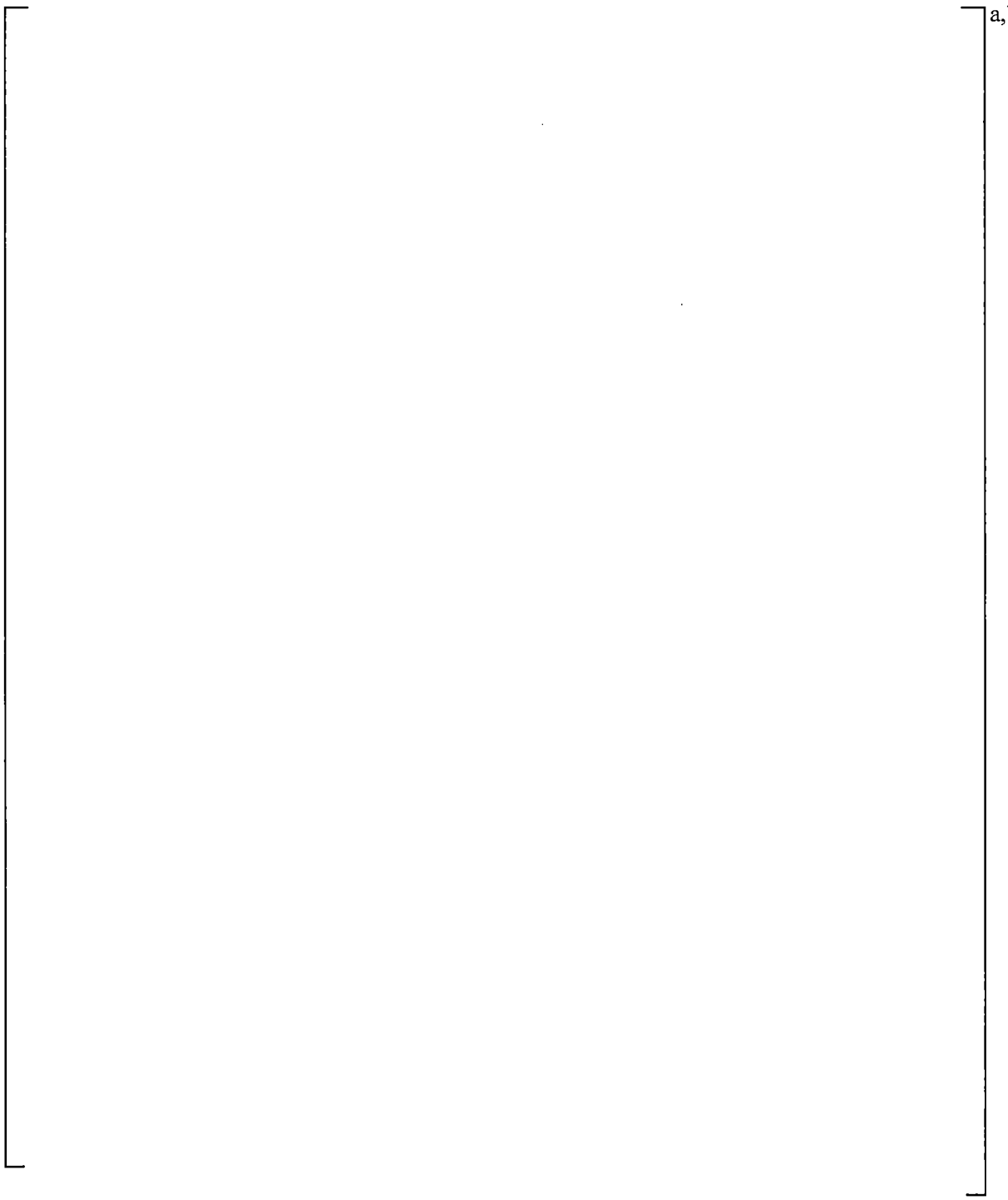

]

Figure 6-1 [ ][a,c]

[ ]a,c

Figure 6-2 [ ]a,c

a,c

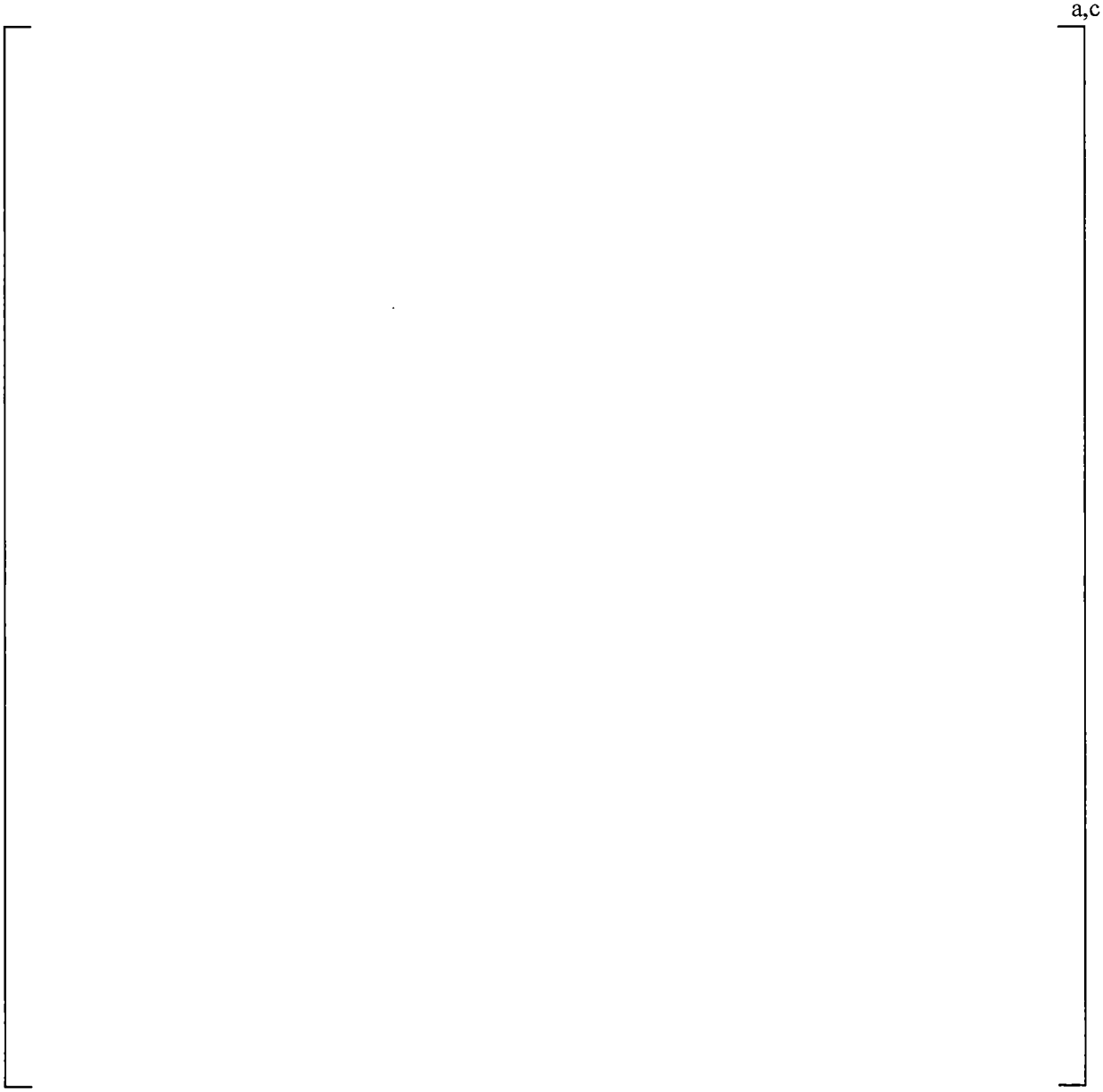

Figure 6-3 [ ][a,c]

a,c

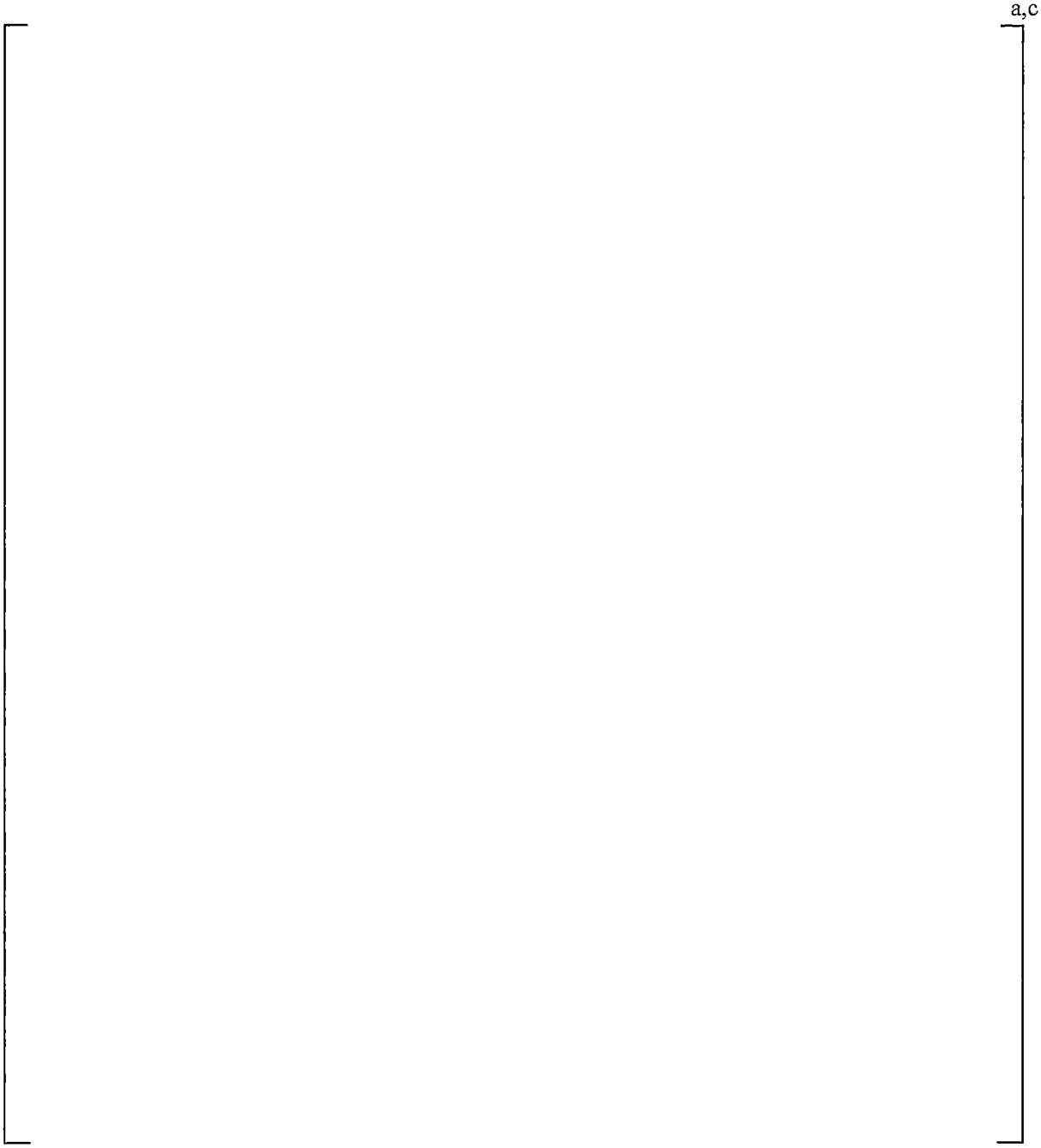

Figure 6-4 [**]**[a,c]

7 STRUCTURAL ANALYSIS

7.1 HARMONIC ANALYSIS

7.1.1 [ ]^{a,c}

Harmonic solutions are obtained using the ANSYS Monticello replacement FEM for the following sets of conditions:

- **Model Support (Boundary) Conditions**

  The model is supported [

  ]^{a,c}.

- **Operating Conditions**

  EPU operating conditions are evaluated.

- **Frequency Shifts**

  [

]^{a,c}.

7.1.2 Overview – Time-History Solution

The harmonic analysis begins with the [

]^{a,c}. As discussed above, separate solutions are obtained for [ ]^{a,c}

[

]^{a,c}.

[

]^{a,c}.

[

]^{a,c}.

It was found to be inefficient to process the results [

]^{a,c}.

[

]^{a,c}.

[

]^{a,c}.

7.1.3 Inverse Fourier Transform

[

]^{a,c}

[

]^{a,c}.

7.1.4 Frequency Scaling (Shifting)

As a result of approximations of the structural interactions used in developing the FEM, small errors can result in the prediction of the component natural frequencies. Varying degrees of mesh discretization can also introduce small errors in the FEM results. To account for these effects, frequency scaling is applied to the applied load history.

If frequency scaling is applied, [

]^{a,c}

7.2 POST-PROCESSING

7.2.1 Primary Stress Evaluation

Once the time-history has been calculated [ ]^{a,c}, an evaluation is performed to calculate the maximum alternating stress intensity. The stress intensities for the [

]^{a,c}.

For a two-dimensional stress field, the principal stresses are calculated as follows (the X-Y plane is used as an example. The same algorithms are also applicable to other planes.)

$$\sigma_{1,2} = \frac{\sigma_x + \sigma_y}{2} \pm \sqrt{\left(\frac{\sigma_x - \sigma_y}{2}\right)^2 + \left(\sigma_{xy}^2\right)}$$

$$\sigma_3 = 0.0$$

$$\text{Stress Intensity} = \text{Maximum} \begin{vmatrix} |\sigma_1 - \sigma_2| \\ |\sigma_2 - \sigma_3| \\ |\sigma_3 - \sigma_1| \end{vmatrix}$$

For a general 3-D state of stress, the resulting principal stresses correspond to the roots of the following cubic equation as:

$$\sigma^3 - a_2\sigma^2 + a_1\sigma - a_0 = 0$$

where,

$$a_2 = \sigma_x + \sigma_y + \sigma_z$$
$$a_1 = \sigma_x\sigma_y + \sigma_y\sigma_z + \sigma_z\sigma_x - \sigma_{xy}^2 - \sigma_{yz}^2 - \sigma_{zx}^2$$
$$a_0 = \sigma_x\sigma_y\sigma_z + 2\sigma_{xy}\sigma_{yz}\sigma_{zx} - \sigma_x\sigma_{yz}^2 - \sigma_y\sigma_{zx}^2 - \sigma_z\sigma_{xy}^2$$

7.2.2 Alternating Stress

The calculation of the alternating stress intensity, following the ASME B&PV Code, Section III, Division 1 – NG process, is performed as follows:

1. Apply the stress concentration factors (geometric or FSRF), as applicable, to the component stresses.

2. Calculate the range of stress for each component of stress for two time points.

3. Calculate the stress intensity of the component ranges.

[

]^{a,c}

[

]^{a,c}.

7.3 CALCULATION AND EVALUATION OF WELD STRESSES

Due to the nature of the dynamic analysis, detailed modeling of the welds is not practical in the global dryer FEM. Calculation of weld stresses requires a different approach. For the Monticello replacement steam dryer, [

]^{a,c}.

As discussed above, detailed weld stresses are not directly available from the finite element analysis.
[

]^{a,c}.

[

]a,c

[

a,c]

[ ]a,c

[

]a,c.

7.4 SUBMODELING TECHNIQUES

Due to the nature of the acoustic analysis and the large number of unit solutions that are required, it is not practical to use a fine mesh for the acoustic structural analysis. Rather a mesh density that can accurately predict the dynamic characteristics of the structure is used, but may require some additional analysis for localized regions of high stress. For areas where additional analysis is necessary using a more refined element mesh, a technique known as submodeling is used. The submodeling method [

]a,c.

7.5 [ ]^{a,c}

[

]^{a,c}.

8 ANALYSIS RESULTS

8.1 GLOBAL MODEL

As discussed previously, [

]^{a,c}.

A summary [

]^{a,c}

8.2 SUBMODELING

Based on the results for the global model, [

]^{a,c}.

8.2.1 [ ]^{a,c}

[

]^{a,c}

8.2.2 Submodel Mesh Density

To demonstrate that the [ ]^{a,c} submodel results are appropriate, [

]^{a,c} The comparison and results are documented in Appendix A of this report.

8.3 ASME ALTERNATING STRESS CALCULATIONS

Section 7.2.2 discusses the [

]^{a,c}

Table 8-1 Summary of Results at EPU: Components [ ]^{a,c}

a,b,c

Table 8-2 Summary of Results at EPU: Components [ ]^{a,c}

a,b,c

Table 8-3 ASME Alternating Stress Calculation Summary

a,b,c

a,c

[

]

Figure 8-1 [ ][a,c]

a,c

[ ]

Figure 8-2 [ ]^{a,c}

a,b,c

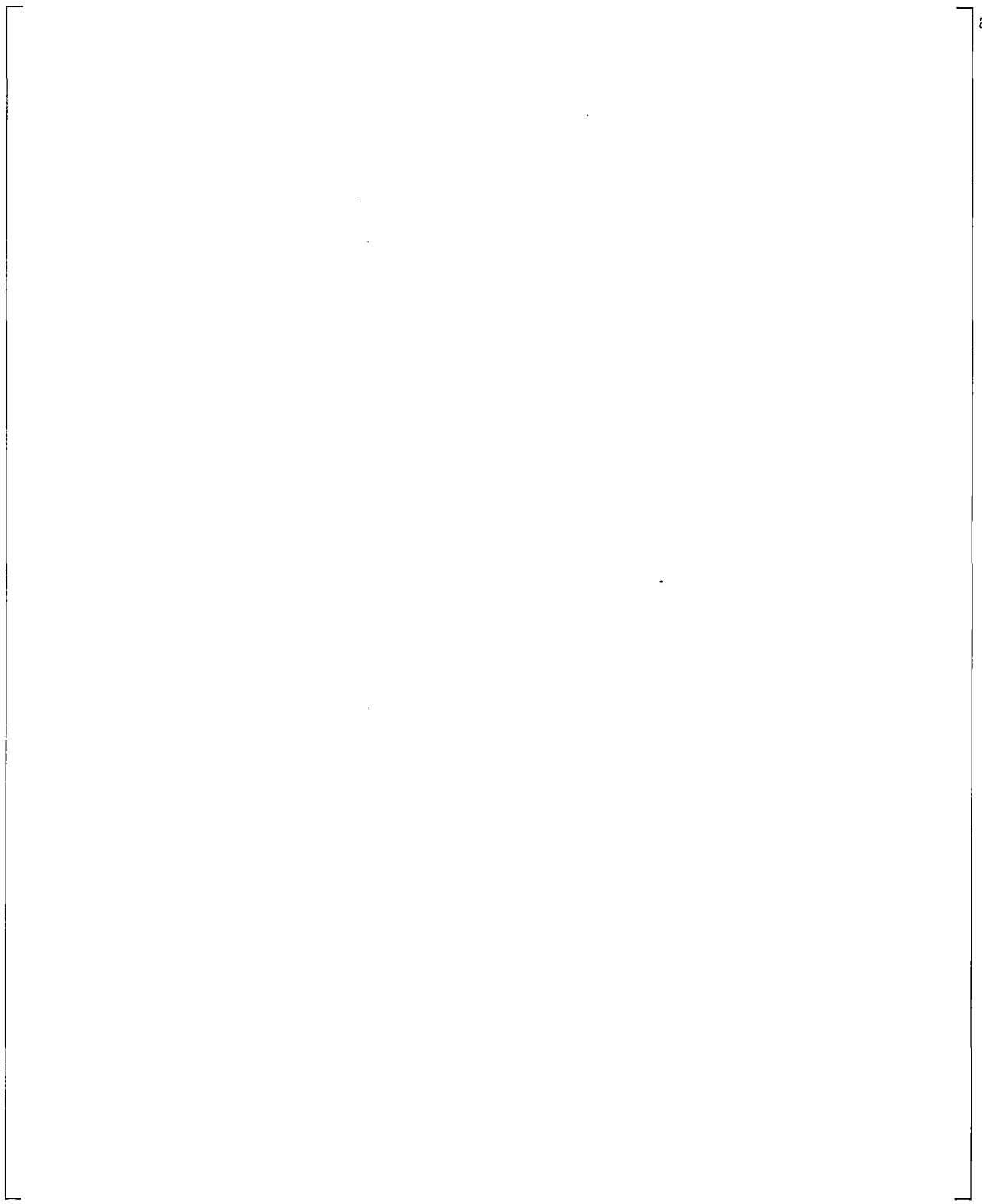

Figure 8-3 [ ][a,c]

[a,b,c

Figure 8-4 [ ][a,c]

[a,b,c

]

Figure 8-5 [ ][a,c]

a,b,c

Figure 8-6 [**]**[a,c]

9 SUMMARY OF RESULTS AND CONCLUSIONS

[

]^{a,c}

The results from these tables for above and below the steam dryer support ring show that the smallest fatigue stress ratios are as follows:

	Above Support Ring	Below Support Ring
Licensing Based Evaluation (based on 2011 CLTP data)	[ ]^{a,c}	[ ]^{a,c}
Power Ascension Test Results Evaluation (based on 2015 EPU data)	[ ]^{a,c}	[ ]^{a,c}

10 REFERENCES

1. ASME Boiler and Pressure Vessel Code, 2004 Edition, Section III, Division 1.
2. ASME Boiler and Pressure Vessel Code, 2004 Edition, Section II, Part D.
3. U.S. Nuclear Regulatory Commission, Regulatory Guide 1.20, Rev. 3, "Comprehensive Vibration Assessment Program for Reactor Internals During Preoperational and Initial Startup Testing," March 2007.
4. [

   ]^{a,c}
5. [

   ]^{a,c}
6. [

   ]^{a,c}
7. BWR Vessel and Internals Project, Guidance for Demonstration of Steam Dryer Integrity for Power Uprate. Electric Power Research Institute, Palo Alto, CA: May 2010. BWR-182-A.
8. [

   ]^{a,c}

APPENDIX A SKIRT SLOT SUBMODEL MESH DENSITY STUDY

To illustrate that the submodel results used are appropriate, [

]^{a,c}

Table A-1 Submodel Cut Boundary Stress Comparison

a,b,c

Table A-2 Submodel Cut Boundary Stress Comparison

a,b,c

[a,b,c

]

Figure A-1 Submodel [ ][a,c]

[a,b,c]

Figure A-2 Submodel Mesh Densities

a,b,c

Figure A-3 [ ]^{a,c} Submodel Results

a,b,c

Figure A-4 [ ]^{a,c} Submodel Results

Figure A-5 [ ]^{a,c} Submodel Results

APPENDIX B HIGH CYCLE FATIGUE STRESS RE-EVALUATION

The recently obtained plant data at 2004 MWt were transmitted from Xcel Energy to Westinghouse on June 30, 2015. Appendix B documents the updated high-cycle fatigue stress ratios that were evaluated from this latest plant EPU data.

This re-evaluation includes [

]^{a,c}

Figure B-1, Figure B-2 and Figure B-3 [

]^{a,c} A summary [

]^{a,c}

[

]^{a,c}

[a,b,c]

Figure B-1 Outer Hood (non-weld)

Figure B-2 Outer Hood to Cover Plate Weld

Figure B-3 Skirt to Skirt Flange Weld

Table B–1 Summary of Results at 2015 EPU: Components Above the Support Ring a,b,c

Table B–2 Summary of Results at 2015 EPU: Components Below the Support Ring a,b,c